Mechanistic Role of Lewis Bases and Other Additives in Quasiliving Carbocationic Polymerization of Isobutylene

Robson F. Storey,* Christopher L. Curry, and L. Krystin Hendry

The University of Southern Mississippi, School of Polymers and High Performance Materials, Box 10076, Hattiesburg, Mississippi 39406-0076

Received September 25, 2000

ABSTRACT: Isobutylene was initiated using 5-*tert*-butyl-1,3-di(2-chloro-2-propyl)benzene/$TiCl_4$ in 60/40 hexane/methyl chloride: $[IB]_0$ = 1.0 M, $[TiCl_4]$ = 0.12 or 0.24 M, [*t*-Bu-*m*-DCC] = 0.0119 M, T = −(40−80) °C. Most polymerizations contained a Lewis base or other additive, i.e., 2,4-dimethylpyridine, 2,6-di-*tert*-butylpyridine, tetra-*n*-butylammonium chloride, and/or pyridine hydrochloride. Polymerizations containing an additive yielded theoretical molecular weights, narrow polydispersity index, and apparent absence of irreversible chain termination (linear kinetic plots, ATR−FTIR spectroscopic data) and chain transfer, with two exceptions: coupled product was obtained at −40 °C, and protic initiation occurred with *n*-Bu_4NCl alone. Polymerizations without an additive produced bimodal molecular weight distributions; however, essentially all chains were initiated from *t*-Bu-*m*-DCC. With an additive, E_{act} for propagation was −(5.3−5.5) kcal/mol. Removal of additives increased polymerization rate moderately at −80 °C but dramatically at −60 and −40 °C; this yielded higher E_{act} compared to that of systems containing additives. These results indicated that both paired and unpaired (free) ions are propagating species in absence of additives, with free ions less important at lower temperatures; free ion concentration and lifetime suggested the presence of adventitious common ions and chain transfer between free ions and *tert*-chloride-terminated PIB chains. The primary role of additives is suppression of free ions through in situ production, via the scavenging of protic impurities, of common ions.

Introduction

Polyisobutylene (PIB) is an industrially important polymer that is obtainable solely through carbocationic polymerization. A little over a decade ago, conditions were discovered whereby the polymerization of isobutylene (IB) could be initiated in a controlled fashion, yielding living polymers with narrow polydisperisity index (PDI).[1−3] It was soon postulated that these polymerizations are not really living, but quasiliving,[4] which denotes existence of an ionization equilibrium between reversibly terminated (dormant) chains possessing *tert*-chloride end groups and actively propagating carbocations (Scheme 1). For IB, the particular conditions that transform conventional, uncontrolled carbocationic polymerizations into quasiliving systems usually involve either $TiCl_4$ or BCl_3 as co-initiator, solvents (or solvent mixtures) of medium to low polarity, relatively low reaction temperatures, and the presence of Lewis base additives including nucleophiles and proton traps.

Both living and quasiliving polymerizations are ideal cases, and real systems approach the ideal more or less closely. The degree of livingness within a particular polymerization may be ranked quantitatively on the basis of the ratios of rate constants of chain transfer and termination (or other chain breaking events) to that of propagation (i.e., k_{tr}/k_p or k_t/k_p).[5] For a quasiliving system with finite k_t/k_p, particularly when this quantity is relatively large, a low ionization equilibrium constant makes the apparent degree of livingness seem higher because it increases the effective lifetime of the polymerization reaction and thereby provides increased time for practical synthetic manipulations.[6]

Several mechanistic theories have been advanced to describe the changes that occur when conventional carbocationic systems are converted to quasiliving

Scheme 1. Ionization Equilibrium between Dormant *tert*-Chloride Chain Ends and Actively Propagating Carbocations

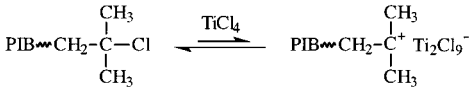

polymerizations via the addition of additives. One of the earlier concepts, so-called "carbocation stabilization", holds that Lewis bases (electron donors) and/or their complexes with Lewis acid interact with the growing chain end to reduce its "cationicity" (i.e., degree of ionization and/or degree of separation between carbocation and counterion) and, moreover, that the reduction in cationicity significantly decreases the polymerization rate, suppresses chain transfer and termination reactions, and narrows the product PDI.[3,7−9] In a recent review, Iván[10] emphasized that only electron donor/Lewis acid complexes, and not electron donors themselves, interact with the carbocations and that this interaction forms a propagating center with reduced reactivity. Plesch has interpreted the role of Lewis base additives in terms of a psuedo-cationic polymerization mechanism.[11] According to this author, the Lewis acid is a "positive modifier" that coordinates with the terminal ester (chloride) group, and the Lewis base is a "negative modifier" that coordinates to the acidic β-protons on the ultimate repeat unit of the propagating chain end. In this interpretation, apparently, the two modifiers balance the reactivity of the strictly covalent chain end and thereby facilitate monomer insertion via a 6-centered cyclic transition state. The characteristic feature of this mechanism is the predominance of the activated ester, rather than the ion pair, in propagation. Penczek[12] has hypothesized that the Lewis base lowers the activation energy for ionization of the covalent species (ester, chloride, etc.) by causing ionization to

10.1021/ma0016432 CCC: $20.00
Published on Web 07/04/2001

proceed through an intermediate onium ion. He proposed that the Lewis base attacks the backside of the halide (or ester), creating onium and halide ions. The latter reacts with Lewis acid to form the counterion, and the onium ion decomposes to form the carbenium ion that is active in propagation. All of the above-discussed interpretations involve σ-bonding of a nucleophilic additive with various electrophilic sites associated with the active chain end. The principal deficiency of these theories is that nonnucleophilic proton traps[13,14] and nonbasic salts such as tetraalkylammonium halides,[15−19] which cannot take part in the proposed mechanisms, also yield quasiliving polymerizations. In fact, as we will show, these nonnucleophilic and nonbasic additives yield results that are virtually indistinguishable from those obtained using nucleophiles; i.e., the kinetics and energetics of polymerization and the structure, molecular weights, and PDIs of the products are essentially identical.

As a counterpoint to the theories above, Matyjaszewski et al.[20,21] and Szwarc[6] have ascribed the "apparent" stabilization of the growing chain ends to a reduction in the instantaneous carbocation concentration, instead of a modification in the structure and reactivity of the active species itself. In their view, living cationic polymerizations do not proceed by a new mechanism, but rather are the result of control of the reaction kinetics through proper selection of polymerization components, initiator concentration, and temperature. Similarly, Faust et al.[13,14] have attributed living behavior to the removal of protic impurities by externally added electron donors. In their view, synthetic control is achieved through the elimination of "induced" chain transfer while maintaining only reversible termination. The proton-scavenging theory of Faust and co-workers was a direct refutation of carbocationic stabilization and was advanced primarily due to the observed effectiveness of the hindered base 2,6-di-*tert*-butylpyridine (D*t*BP) in bringing about living behavior. D*t*BP is widely thought to be unable to complex with Lewis acids, and thus it was reasoned that it could not participate in any stabilizing interactions with carbocations. Other investigations have revealed that unpaired (free) ions do not participate as chain carriers within IB polymerizations mediated by nucleophilic additives or proton traps;[22,23] also, as mentioned above, conventional carbocationic polymerizations have been converted to quasiliving systems through the exclusive use of common ion salt precursors such as *n*-Bu_4NCl,[15−19] *n*-Bu_4NI,[19] or crown-16-ether in conjunction with KCl.[24] These facts suggest that nonliving behavior may be simply attributed to uncontrolled propagation by dissociated, free carbocations. From the foregoing, it is clear that controversy exists within the carbocationic polymerization community regarding the precise role of additives in bringing about quasiliving behavior in polymerizations.

Other inquiries have been reported as well, including investigations on the mechanism of initiation,[25,26] determination of rate constants of the individual elementary reactions involved,[27−29] determination of the kinetic order of propagation with respect to Lewis acid,[22,30−34] and characterization of side reactions that cause deviations from ideal living behavior.[35,36−38] Recently, we discovered that the dominant chain-interrupting event in $TiCl_4$-*co*-initiated IB polymerizations is a complex combination of carbenium ion rearrangement and β-proton transfer to the counterion or to a proton trap, if present.[35,39] The relative rates of the various chain-breaking events were dependent on both [$TiCl_4$] and Lewis base identity and concentration;[39] therefore, a more complete understanding of the physical/chemical state of the active chain carriers within these polymerizations was needed to interpret the mechanism of chain rearrangement/termination. To relate the rates of these chain-breaking events to that of propagation, we measured propagation kinetics under the same conditions, i.e., those that yield products of low molecular weight to facilitate end group analysis and high rates to promote completion of chain-end degradation processes within reasonable times. This paper reports the results of our study of propagation kinetics, including comparison of the structure and reactivity of propagating chains in both conventional (no additives) and quasiliving IB polymerizations, with particular attention given to elucidating the mechanism by which additives convert the former into the latter.

Experimental Section

Materials. The preparation of 5-*tert*-butyl-1,3-bis(2-chloro-2-propyl)benzene (*t*-Bu-*m*-DCC) has been previously reported.[30] Hexane (Hex) (95+%, Aldrich Chemical Co.) was dried prior to use by distillation from CaH_2. IB and CH_3Cl (MeCl) (both BOC, 99.5%) were dried through columns packed with $CaSO_4$ and $CaSO_4$/4 Å molecular sieves, respectively. $TiCl_4$ (99.9%, Aldrich Chemical Co., packaged under N_2 in SureSeal bottles) was refluxed over copper filings under N_2 and then vacuum-distilled into dry glass ampules.[40] 2,4-Dimethylpyridine (DMP) and 2,6-di-*tert*-butylpyridine (D*t*BP) (both Aldrich Chemical Co.) were distilled from CaH_2 under reduced pressure into dry, glass ampules (final purity by GC 99.9+% for both Lewis bases). All ampules were sealed under vacuum and stored at 0 °C until just prior to use. Tetra-*n*-butylammonium chloride (*n*-Bu_4NCl, 99+%), pyridine hydrochloride (Pyr-HCl, 98%), and anhydrous methanol (MeOH, 99.8%) were used as received from Aldrich Chemical Co.

Instrumentation. Molecular weights and molecular weight distributions were determined using a gel permeation chromatography (GPC) system equipped with a Waters Alliance 2690 separation module, a Waters 484 tunable absorbance detector operating at 265 nm, an on-line multiangle laser light scattering (MALLS) detector operating at 690 nm (MiniDawn, Wyatt Technology Inc.), an interferometric refractometer (Optilab DSP, Wyatt Technology Inc.) operating at 35 °C, and two PLgel GPC columns (Polymer Laboratories Inc.) connected in series. For characterization of monomodal products, two mixed E columns (pore size range 50−10^3 Å, 3 μm bead size) were used; for bimodal products, two mixed D columns (pore size range 50−10^4 Å, 5 μm bead size) were used. THF was used as the mobile phase at a flow rate of 1 mL/min. Sample concentrations were approximately 5−10 mg/mL in freshly distilled THF, with an injection volume of 100 μL. Detector signals were simultaneously recorded, and absolute molecular weights and PDIs were calculated using ASTRA software (Wyatt Technology Inc.). A d*n*/d*c* value of 0.107 mL/g was used for PIB in THF. Peak deconvolution/fitting of RI and UV chromatograms was performed using Grams/32 peak-fitting software. Chromatograms were fitted to a mixed Gaussian/Lorentzian curve, with fitting iterations performed until a χ^2 value ≤ 1 was reached.

Solution ^{1}H NMR spectra were obtained on a Bruker AC-300 spectrometer using 5 mm o.d. tubes with sample concentrations of 5−15% (w/v) in deuterated chloroform ($CDCl_3$) (Aldrich Chemical Co.) containing tetramethylsilane as an internal reference.

A ReactIR 1000 reaction analysis system (light conduit type) (ASI Applied Systems, Millersville, MD), equipped with a DiComp (diamond composite) insertion probe, a general-purpose type PR-11 platinum resistance thermometer, and CN76000 series temperature controller (Omega Engineering,

Stamford, CT), was used to collect infrared spectra of the polymerization components and monitor reactor temperature in real time as previously described.[41]

Polymerization and ATR−FTIR Data Collection Procedure. Polymerizations were carried out under dry nitrogen gas in a Mbraun Labmaster 130 glovebox, equipped with an integral heptane bath cooled by both a FTS RC210 recirculating chiller (FTS Systems) and liquid nitrogen, the latter regulated by a CN76000 series temperature controller (Omega Engineering).

The rapid acquisition mode of the ReactIR 1000 was utilized to collect ATR−FTIR data during reagent addition and subsequent polymerization of the isobutylene. Each spectrum was the Fourier transformation of 2−32 acquisitions collected over the spectral ranges 4000−2200 and 1900−650 cm^{-1}, with an instrument resolution of 8 cm^{-1}.[25] The IB absorbance at a given time was determined by measuring the peak height at 887 cm^{-1}, referenced to a two-point baseline. The absorbance for isobutylene at 887 cm^{-1} decreases with increasing temperature by a factor of 0.42%/°C;[25] the data were corrected by this factor when the reactor temperature rose above the nominal polymerization temperature due to polymerization exotherm. Thus, characteristic absorbance vs time profiles were generated and converted to relative IB concentrations using the following relationship:

$$\frac{[\mathrm{IB}]_0}{[\mathrm{IB}]_t} = \frac{A_0 - A_b}{(A_t - A_b)(1 + 0.0042\Delta T)} \quad (1)$$

where A_b is the average value of the baseline absorbance at $t = \infty$, after complete reaction of the monomer. A_0 is the average absorbance of the reaction solution before the introduction of the co-initiator $TiCl_4$ and is proportional to the initial monomer concentration, $[IB]_0$. $[IB]_t$ and A_t are the monomer concentration and absorbance, respectively, at time t, and ΔT is the difference between the actual temperature of the reactor contents, measured by a platinum resistance thermometer, and the nominal temperature of the experiment.

IB Polymerization Kinetics. Polymerizations were performed at temperatures of −80, −70, −60, and −40 °C. The nominal $TiCl_4$ concentration ($[TiCl_4]_{nom}$) was varied as 0.12 and 0.24 M for each reaction temperature and additive used. The additive concentration ranges utilized were [DMP] = [D*t*BP] = 2.5×10^{-3} M, [*n*-Bu_4NCl] = $(2.7-18.2) \times 10^{-3}$ M, and [Pyr-HCl] = 4.3×10^{-3} M; [*t*-Bu-*m*-DCC]$_0$ = $(0.617-11.9) \times 10^{-3}$ M. The following reaction conditions were held constant: reaction volume = 0.2 L; $[IB]_0$ = 1.0 M. Table 1 lists specific recipes used for the various polymerizations. A representative experimental procedure was as follows: the DiComp probe was sheathed within a stainless steel scabbard, submerged within the −80 °C heptane bath, and allowed to reach thermal equilibrium. An air background spectrum was then obtained by averaging 1024 scans at a resolution of 8 cm^{-1}; this spectrum was subtracted from all subsequent spectra to correct for absorbances due to the DiComp probe. The heptane bath was partially drained, and the scabbard was removed. A 250 mL four-neck round-bottom flask equipped with a mechanical stirrer and platinum resistance thermometer was placed around the probe, and the heptane bath was raised and allowed to return to −80 °C. The flask was charged with 2.38×10^{-3} mol (0.682 g) of *t*-Bu-*m*-DCC, 110.5 mL of Hex, 73.7 mL of MeCl, 5.0×10^{-4} mol (57.8 μL) of DMP, and 0.20 mol (15.8 mL) of chilled IB (−80 °C). The reaction mixture was stirred until the solution reached thermal equilibrium as indicated by the platinum resistance thermometer, and then 0.024 mol (2.61 mL) of $TiCl_4$ (neat and at room temperature) was rapidly injected into the reactor. Using a chilled Pasteur pipet, polymer samples for GPC and NMR analysis were obtained at various reaction times by withdrawing 1−2 mL aliquots from the reaction vessel and immediately adding them to separate scintillation vials containing 10 mL of anhydrous MeOH.

Table 1. Isobutylene Polymerization Recipes Utilizing Common Ion Salt and/or Lewis Base[a]

temp (°C)	$[TiCl_4]_{nom}$ (M)	[*n*-Bu_4NCl] × 10^3 (M)	[DMP] × 10^3 (M)	[D*t*BP] × 10^3 (M)
−80	0.12	-	2.50	-
		5.40	2.50	-
		-	-	2.50
		5.40	-	2.50
		5.40	-	-
	0.24	-	2.50	-
		-	-	2.50
−70	0.12	-	2.50	-
		-	-	2.50
		2.7	-	-
		4.1	-	-
		8.1	-	-
		18.2	-	-
	0.24	-	2.50	-
		-	-	2.50
−60	0.12	-	2.50	-
		5.40	2.50	-
		-	-	2.50
		5.40	-	2.50
		5.40	-	-
	0.24	-	2.50	-
		-	-	2.50
−40	0.12	-	2.50	-
		5.40	2.50	-
		-	-	2.50
		5.40	-	2.50
		5.40	-	-
	0.24	-	2.50	-
		-	-	2.50

[a] Reaction conditions: $[IB]_0$ = 1.0 M; [*t*-Bu-*m*-DCC]$_0$ = 1.19×10^{-2} M; 60/40 Hex/MeCl cosolvents (v/v).

Results and Discussion

IB polymerizations were performed to compare four different reaction variables: initiator concentration, type and concentration of additive (i.e., DMP, D*t*BP, *n*-Bu_4NCl, or Pyr-HCl), co-initiator concentration ($[TiCl_4]_{nom}$), and polymerization temperature. Additional polymerizations were conducted in the absence of any additive (conventional polymerizations) at varying initiator concentrations and polymerization temperatures. To minimize the introduction of contaminants, the Lewis acid was rigorously purified and stored in sealed ampules until just prior to use. A difunctional aromatic initiator was used, and most of the polymerizations were designed with a relatively low monomer/chain end ratio of 42. These conditions yield oligomeric PIB that is amenable to end group characterization via ^1H and ^{13}C NMR, and it provides a single UV-active initiator fragment per chain that is accurately quantified using GPC with UV detection. This relatively high initiator concentration yields fast reactions whose kinetics, although difficult to measure gravimetrically, were easily measured using real-time in situ ATR−FTIR spectroscopy, a technique recently developed for these systems by Storey et al.[25,31,41] and Puskas et al.[33,34,42,43]

Effect of Temperature on Lewis Base-Mediated IB Polymerizations. The effect of temperature on the rate of Lewis base-mediated IB polymerizations was investigated by measuring first-order kinetics for polymerizations at −40, −60, −70, and −80 °C while holding concentrations of IB, *t*-Bu-*m*-DCC, and Lewis base constant at 1.0, 1.19×10^{-2}, and 2.5×10^{-3} M, respectively, within a Hex/MeCl (60/40 v/v) cosolvent mixture. Polymerizations were carried out at two nominal $TiCl_4$ concentrations, 0.12 and 0.24 M, utilizing DMP or D*t*BP as the Lewis base. Figure 1 shows

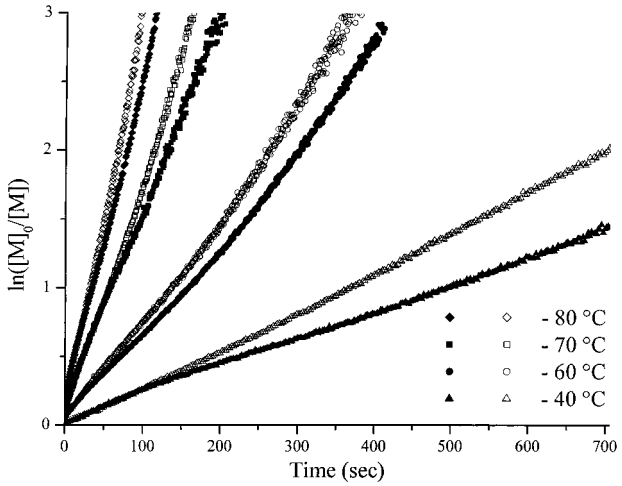

Figure 1. First-order kinetic plots for IB polymerizations at various temperatures. $[IB]_0 = 1.0$ M; [*t*-Bu-*m*-DCC]$_0 = 1.19 \times 10^{-2}$ M; $[TiCl_4]_{nom} = 0.12$ M; 60/40 Hex/MeCl cosolvents (v/v); filled symbols, $[DMP] = 2.5 \times 10^{-3}$ M; open symbols, [D*t*BP] $= 2.5 \times 10^{-3}$ M.

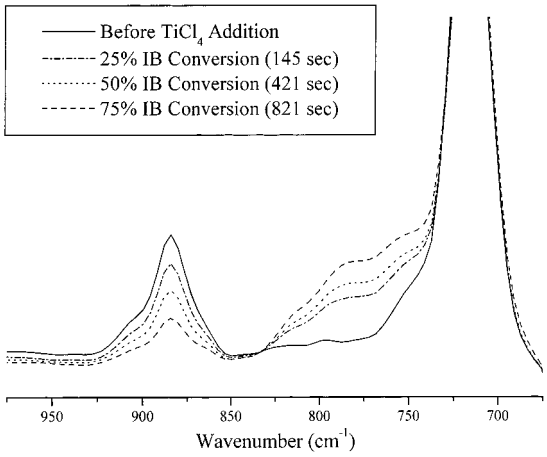

Figure 2. Partial ATR−FTIR spectra of DMP-mediated IB polymerization medium at −40 °C prior to addition of $TiCl_4$ (solid line) and at various IB conversions. $[IB]_0 = 1.0$ M; [*t*-Bu-*m*-DCC]$_0 = 1.19 \times 10^{-2}$ M; $[DMP] = 2.5 \times 10^{-3}$ M; $[TiCl_4]_{nom} = 0.12$ M; 60/40 Hex/MeCl cosolvents (v/v).

semilogarithmic kinetic plots (ln([M]$_0$/[M]) vs time) for the $[TiCl]_{nom} = 0.12$ M data, which are representative. Rate constants, k_{app}'s, for all of the reactions at both Lewis acid concentrations are listed in Table 2.

All of the first-order plots were linear and showed no evidence of irreversible termination, even at the highest temperature studied (Supporting Information, Figure A). Two minor deviations from linearity were observed, however, which are characteristic of this particular system. Most of the first-order plots displayed a slightly higher slope at very short times compared to the rest of the plot, giving the appearance of a positive *y*-intercept. This initial period of rapid monomer consumption has been ascribed to the increased ionization equilibrium constant for the *tert*-benzylic chloride initiator relative to the *tert*-alkyl chloride PIB chain ends.[25] This effect becomes more pronounced with decreasing temperature, in agreement with an earlier paper.[25] In general, the rapid monomer consumption event is much less pronounced within the present regime of $[TiCl_4]_{nom}$ compared to that in the earlier report, which was over an order of magnitude lower. A second minor deviation is the very slight, gradual upward curvature of the plots, most apparent in the −60 °C data in Figure 1. This gradual increase in the apparent rate constant occurs as the initial exotherm of the polymerization reaction is dissipated, and the cooling system reestablishes the correct reactor temperature.

A reviewer suggested that the −40 °C plots in Figure 1 should display downward curvature, since Faust et al.[37] showed that the polymerization of IB is not free of termination at this relatively high temperature. We have addressed this point in detail in an upcoming paper,[36] where we report that approximately 5−6 propagation half-lives would be required before a detectable amount of termination (10%) had occurred at −40 °C under the conditions of Figure 1. The reactions at −40 °C in Figure 1 were conducted to only 2−3 half-lives; thus, termination was not detected. Our systems appear more living than those of Faust et al.[37] principally because our chain-end concentration is over 1 order of magnitude higher.

Several new absorbance bands appeared within the ATR−FTIR spectra of reaction mixtures at −60 and −40 °C, with the most intense of these located at 783 cm^{-1}. This absorbance band was only observed for reaction mixtures containing DMP (Figure 2). Similar findings were reported by Storey and Donnalley, who found that accurate kinetic analysis of $TiCl_4$-*co*-initiated IB polymerizations conducted at temperatures in excess of −60 °C was impeded by the overlap of this new absorbance

Table 2. Apparent First-Order Rate Constants, k_{app}, and Apparent Activation Energies, E_{act}, for the Polymerization of Isobutylene[a]

			$10^3 k_{app}$, s^{-1} at specified temp				
$[TiCl_4]_{nom}$ (M)	additive	[additive(s)] × 10^3 (M)	−40 °C	−60 °C	−70 °C	−80 °C	E_{act} (kcal/mol)
0.12	DMP	2.50	2.20	6.81	14.14	23.29	−5.32
	D*t*BP	2.50	2.91	7.78	17.50	28.62	−5.31
	n-Bu$_4$NCl	2.71			19.79		
		4.06			18.75		
		5.40	2.95	9.64	18.02	32.80	−5.44
		8.13			19.33		
		18.20			17.21		
	Pyr-HCl	4.30			64.84		
	Pyr-HCl[b]	4.30			13.13		
	n-Bu$_4$NCl + DMP	5.40 + 2.50	2.03	6.57		22.71	−5.51
	n-Bu$_4$NCl + D*t*BP	5.40 + 2.50	2.64	7.73		28.57	−5.44
	no additive		26.11	33.05		47.21	
0.24	DMP	2.50	5.07	18.44	34.39	62.20	−5.59
	D*t*BP	2.50	7.09	18.80	43.87	74.10	−5.25

[a] Reaction conditions: $[IB]_0 = 1.0$ M; [*t*-Bu-*m*-DCC]$_0 = 1.19 \times 10^{-2}$ M; 60/40 Hex/MeCl cosolvents (v/v). [b] $TiCl_4$ and Pyr-HCl were added as a solution in MeCl.

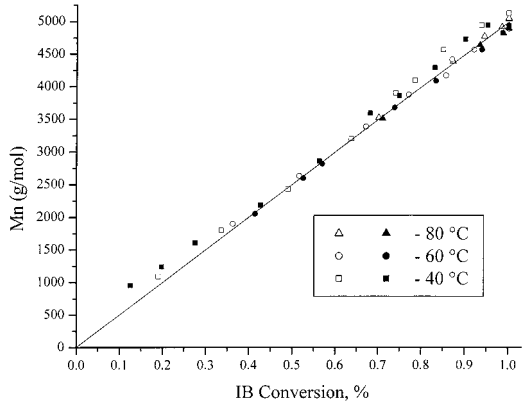

Figure 3. M_n vs monomer conversion plots for IB polymerizations at various reaction temperatures. $[IB]_0 = 1.0$ M; $[t\text{-Bu-}m\text{-DCC}]_0 = 1.19 \times 10^{-2}$ M; $[TiCl_4]_{nom} = 0.12$ M; 60/40 Hex/MeCl cosolvents (v/v); filled symbols, $[DMP] = 2.5 \times 10^{-3}$ M; open symbols, $[DtBP] = 2.5 \times 10^{-3}$ M. Line is theoretical.

with the $=CH_2$ wag of IB at 887 cm^{-1}.[25] Although this absorbance increases in intensity with increasing reaction time and temperature, it did not significantly interfere with the 887 cm^{-1} band used to monitor IB decay in any of the polymerizations performed in this study. We speculate that this absorbance is due to insoluble $TiCl_4$:DMP complex that gradually plates onto the diamond-composite probe surface at higher temperatures; moreover, as polymerization temperature is lowered, the solubility of this complex increases, thus reducing the amount of plating onto the probe. Since the $TiCl_4$ concentration used by Storey and Donnalley was approximately an order of magnitude lower than in the present study, the fact that these authors reported a much more intense absorbance at 783 cm^{-1} suggests that the solubility of the complex is enhanced with increases in $TiCl_4$ concentration. Since no distinct absorbance bands were noted at 783 cm^{-1} within the spectra of D*t*BP-mediated IB polymerizations (Supporting Information, Figure B), we assume that either there is no complex formed between D*t*BP and $TiCl_4$,[13,14,44] or if a complex does exist,[45,46] it is completely soluble within this particular medium.

M_n (GPC) vs IB conversion (ATR−FTIR monitoring) plots for $[TiCl_4]_{nom} = 0.12$ M are shown in Figure 3. Plots obtained at $[TiCl_4]_{nom} = 0.24$ M were similar. The extremely high rates of the polymerizations performed at −80 and −60 °C did not allow GPC aliquots to be taken at low IB conversions; consequently, the first samples analyzed were at approximately 70% and 35% IB conversion, respectively. Chain transfer is largely absent as demonstrated by the linearity of the plots and the close agreement of the data with the theoretical line. PDIs of the aliquots decreased with conversion, starting at about 1.7−1.8 for the earlier aliquots (≤35% conversion) (Supporting Information, Figure C). Regardless of polymerization temperature or $[TiCl_4]$, the final (≈98% conversion) PIBs produced in the presence of either Lewis base were all monomodal with narrow PDI (1.02−1.05). In general, at a given conversion PDIs increased slightly with decreasing temperature (Supporting Information, Figure D). This is caused by increasing propagation run number (i.e., the average number of monomer units added to a chain per ionization period[23,25,28]) with decreasing temperature.

Aliquots removed from the −80 °C polymerizations exhibited monomodal peaks in GPC analysis and a

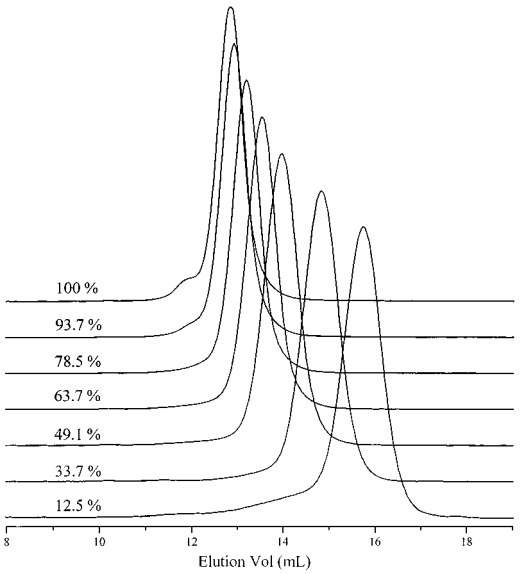

Figure 4. GPC chromatograms for D*t*BP-mediated IB polymerization at −40 °C at varying IB conversions (labeled above each trace). $[IB]_0 = 1.0$ M; $[t\text{-Bu-}m\text{-DCC}]_0 = 1.19 \times 10^{-2}$ M; $[DtBP] = 2.5 \times 10^{-3}$ M; $[TiCl_4]_{nom} = 0.12$ M; 60/40 Hex/MeCl cosolvents (v/v).

linear increase in M_n throughout the range of IB conversions sampled, for both Lewis bases and $TiCl_4$ concentrations studied. At −60 and especially at −40 °C, however, a broad shoulder was observed on the leading edge (low elution volume side) of GPC chromatograms of aliquots taken during the early stages of polymer growth (i.e., ≤35% conversion), for both DMP and D*t*BP. This shoulder is clearly visible in Figure 4 for the 12.5% conversion aliquot of the −40 °C polymerization conducted in the presence of D*t*BP. Moreover, it was visible in both the RI and UV traces, indicating that this high molar mass fraction contains the aromatic *t*-Bu-*m*-DCC initiator fragment and eliminating the possibility that it represents initiation by adventitious moisture. As will be discussed in the ensuing section, this shoulder is ascribed to a transient fraction of unpaired (free) carbocations that propagate prior to the formation of excess $[Ti_2Cl_9^-]$ anions via the proton scavenging function of the Lewis base. We further hypothesize that this shoulder would also be observed at −80 °C (and at −60 °C for polymerizations utilizing $[TiCl_4]_{nom} = 0.24$ M) if an experiment were designed to collect aliquots at such short times.

Returning to Figure 3, the −40 °C polymerizations produced data points that were above the theoretical line at the very lowest and very highest conversions. Elevation of the low-conversion points above the theoretical line is probably caused by the well-known overestimation of molecular weight for very low molecular weight polymers using MALLS and is unrelated to the leading shoulder in GPC chromatograms discussed above. Elevation of the high-conversion points (≥70% conversion) above the line is caused by a small fraction of chain-coupled polymers, clearly visible in Figure 4, especially for the 93.7 and 100% traces, as a narrow shoulder at an elution volume corresponding to twice the targeted M_n. Chain coupling results when a propagating carbocation reacts with olefin-terminated PIB. The latter is formed by terminative chain transfer (β-proton transfer to the Lewis base), which may be either unimolecular (transfer occurring first to the counterion) or the result of abstraction by free (i.e.,

uncomplexed) Lewis base. Recent reports from our laboratory and others have shown that IB polymerizations performed at higher polymerization temperatures undergo unimolecular β-proton elimination[37,39] and/or nucleophilic proton abstraction.[39] The RI GPC chromatograms at complete conversion at −40 °C revealed a chain-coupled mass fraction of 5.7 and 2.3% for D*t*BP- and DMP-mediated polymerizations, respectively. The enhanced degree of chain coupling seen for D*t*BP-mediated systems suggests that its participation in β-proton abstraction is greater than for DMP.

An analytical technique utilizing GPC developed by Kennedy et al.,[47] and later refined by Nagy,[48] is an effective diagnostic method to probe the structural homogeneity of polymer molecules containing spectroscopically identifiable functional groups. PIBs prepared using a dicumyl-type initiator contain a UV-active moiety, whose distribution within the polymer chains can be quantified using the simultaneously recorded RI and UV detector data obtained during GPC analysis. Since the heights of the UV and RI traces are proportional to the number of chromophores and mass fraction of sample, respectively, at any given elution volume, the distribution of aromatic moieties within the polymer may be calculated by constructing a plot of

$$y = \frac{(\mathrm{UV/RI})_m}{(\mathrm{UV/RI})_m + (\mathrm{UV/RI})_x} \quad \text{versus} \quad x = \frac{(\mathrm{MW})_x}{(\mathrm{MW})_m + (\mathrm{MW})_x} \quad (2)$$

where $(\mathrm{UV/RI})_m$ and $(\mathrm{MW})_m$ are reference values for the detector response ratio and molecular weight, respectively, taken at some arbitrary reference elution volume, and x denotes (UV/RI) and molecular weight values at various elution volumes. The Kennedy−Smith−Nagy (KSN) plot affirms that, if a slope of unity is obtained with the absence of a y-intercept, then at every elution volume, x, the number of chromophore per macromolecule is constant. Figure 5 shows a representative GPC trace and corresponding KSN plot of a PIB sample that was prepared at a polymerization temperature of −80 °C using DMP, with the reference elution volume for the KSN plot taken at the maximum of the RI trace. In agreement with the findings of Nagy,[48] ambiguous results were obtained for data lying within the outer extremities of the chromatograms (i.e., points at very low detector response); therefore, examinations were confined to those areas bracketed by the shaded regions of the chromatograms in Figure 5. A slope of 1.01 and an intercept value of −0.004 demonstrate that each of the polymer molecules within the distribution contains the same number of aromatic moieties, i.e., one *t*-Bu-*m*-DCC residue. These results confirm the absence of protic initiation and chain transfer events during the polymerization. KSN analysis performed at the various reaction temperatures (Table 3) revealed that all polymerizations carried out in the presence of a Lewis base additive, whether DMP or D*t*BP, yielded PIB molecules of uniform structure that were all initiated from the *t*-Bu-*m*-DCC initiator. The only exception was the small fraction of coupled chains observed with either Lewis base at −40 °C.

Effect of Temperature and Common Ion Salt on IB Polymerizations. The synthesis of polymers with narrow molecular weight distributions requires that the active species within the polymerization system have similar reactivity or that the exchange reactions between the species are rapid when compared to propagation.[23,49] The participation of free ions in propagation can be reduced or eliminated by adding substances capable of forming a common anion, i.e., n-Bu_4NCl. Investigations of BCl_3-*co*-initiated IB polymerizations in polar solvents have shown that addition of a small quantity of n-Bu_4NCl converts conventional IB polymerizations to quasiliving ones, by preventing the formation of the highly reactive free carbocations that are responsible for chain transfer and termination.[15] On the basis of these findings, we decided to investigate the effect of common ion addition to $TiCl_4$-*co*-initiated IB polymerization systems of lower solvent polarity. The effect of temperature and n-Bu_4NCl concentration on the rate of IB polymerizations was investigated by measuring first-order kinetics for polymerizations at −40, −60, −70, and −80 °C while holding concentrations of IB, *t*-Bu-*m*-DCC, and $TiCl_4$ constant at 1.0, 1.19×10^{-2}, and 0.12 M, respectively, within a Hex/MeCl (60/40 v/v) cosolvent mixture.

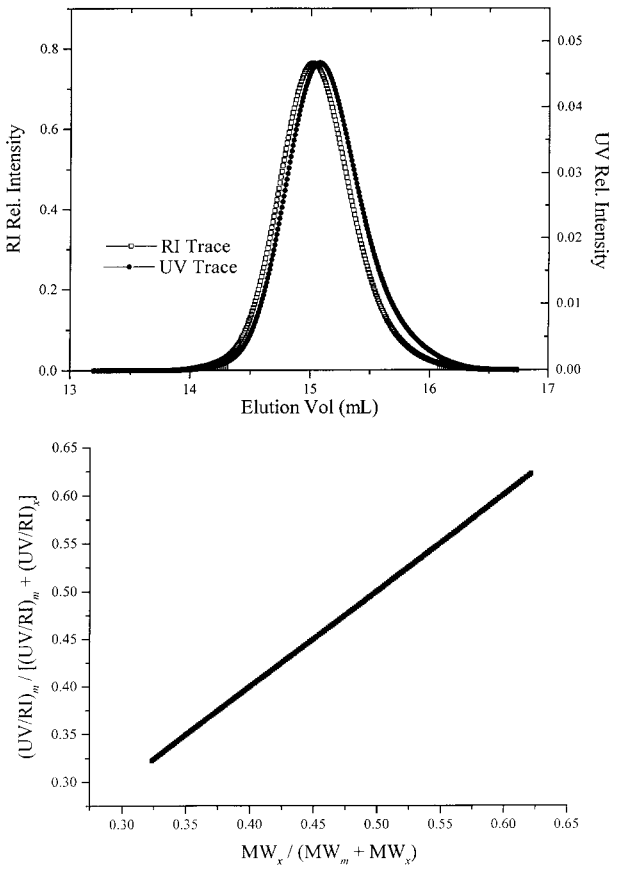

Figure 5. Top: RI and UV GPC traces of PIB produced at −80 °C. $[IB]_0 = 1.0$ M; $[t\text{-Bu-}m\text{-DCC}]_0 = 1.19 \times 10^{-2}$ M; $[TiCl_4]_{nom} = 0.12$ M; $[DMP] = 2.50 \times 10^{-3}$ M; 60/40 Hex/MeCl cosolvents (v/v). Bottom: Kennedy−Smith−Nagy analysis of GPC traces, excluding fractions at very high and low elution volumes (shaded areas in top figure).

The kinetics of polymerizations conducted at the various reaction temperatures using $[n\text{-}Bu_4NCl] = 5.4 \times 10^{-3}$ M were measured. The resulting first-order plots were linear for all temperatures (Figure 6) and virtually indistinguishable from the plots observed for the Lewis base-mediated systems. Just like for the latter systems, a strong decrease in polymerization rate was noted as reaction temperature was increased (k_{app}'s are listed in

Table 3. Quantitative Analysis of RI and UV GPC Traces (Kennedy−Smith−Nagy Method) of PIBs Produced under Quasiliving and Conventional (No Additive) Isobutylene Polymerization Conditions[a]

		KSN analysis		
temp (°C)	additive(s)	discontinuous?	slope 1 (intercept 1)	slope 2 (intercept 2)
−80	DMP	no	1.013 (−0.0041)	
	D*t*BP	no	0.989 (0.0031)	
	n-Bu_4NCl	yes	1.014 (0.0066)	0.995 (0.0025)
	n-Bu_4NCl + DMP	no	0.991 (−0.0023)	
	n-Bu_4NCl + D*t*BP	no	1.105 (−0.0012)	
	no additive	yes	1.20 (−0.0019)	0.999 (0.0028)
−60	DMP	no	1.130 (0.0052)	
	D*t*BP	no	0.993 (−0.0039)	
	n-Bu_4NCl	yes	1.023 (0.0136)	0.994 (0.0029)
	n-Bu_4NCl + DMP	no	1.051 (0.0042)	
	n-Bu_4NCl + D*t*BP	no	1.102 (−0.0013)	
	no additive	yes	1.151 (5.7×10^{-4})	0.998 (0.0041)
−40	DMP	no	0.996 (0.0011)	
	D*t*BP	no	1.019 (−0.0072)	
	n-Bu_4NCl	yes	1.039 (0.0038)	1.015 (−0.0076)
	n-Bu_4NCl + DMP	no	1.103 (−0.0062)	
	n-Bu_4NCl + D*t*BP	no	0.989 (0.0011)	
	no additive	no	0.994 (-7.16×10^{-4})	

[a] Reaction conditions: $[IB]_0 = 1.0$ M; [*t*-Bu-*m*-DCC]$_0 = 1.19 \times 10^{-2}$ M; [*n*-Bu_4NCl] $= 5.4 \times 10^{-3}$ M; [DMP] (or [D*t*BP]) $= 2.5 \times 10^{-3}$ M; $[TiCl_4]_{nom} = 0.12$ M; 60/40 Hex/MeCl cosolvents (v/v).

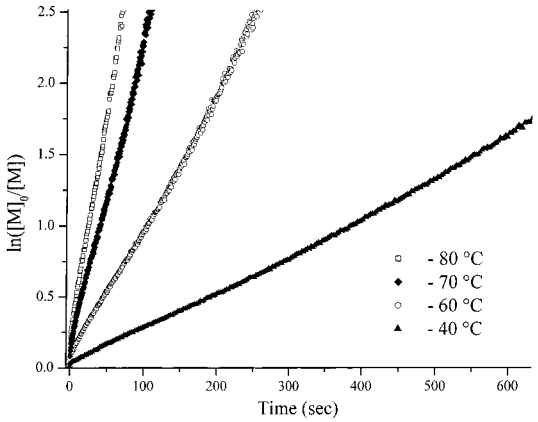

Figure 6. First-order kinetic plots for IB polymerizations at various temperatures. $[IB]_0 = 1.0$ M; [*t*-Bu-*m*-DCC]$_0 = 1.19 \times 10^{-2}$ M; $[TiCl_4]_{nom} = 0.12$ M; 60/40 Hex/MeCl cosolvents (v/v); [*n*-Bu_4NCl] $= 5.4 \times 10^{-3}$ M.

Table 2). Interestingly, the k_{app}'s of *n*-Bu_4NCl-mediated systems were slightly larger in most instances than those for DMP or D*t*BP under otherwise identical conditions. M_n vs monomer conversion plots (Supporting Information, Figure E) were linear throughout the range of IB propagation, with the only deviation from linearity being due to coupling, which occurred only at high IB conversions for polymerizations conducted at −40 °C. The high molecular weight, leading shoulder noted in the initial stages of polymer growth for Lewis base-mediated polymerizations was significantly reduced, but not altogether suppressed, with the use of *n*-Bu_4NCl. Since *n*-Bu_4NCl is not basic, it cannot complex with Lewis acid, nor can it scavenge protons or stabilize carbocations. Its principal role is to provide the system with a surplus of the common anion, $Ti_2Cl_9^-$, via the reaction scheme in eq 3.

$$2TiCl_4 + n\text{-}Bu_4NCl \rightleftharpoons n\text{-}Bu_4N^+ + Ti_2Cl_9^- \quad (3)$$

Thus, these findings suggest that the deviation from livingness noted in conventional IB polymerizations may be largely related to the presence of a fraction of free carbocations. If the concentration of purposefully added initiator is low and the protic impurity concentration is high, then protic initiation might also become important with regard to loss of livingness.

Quantitative GPC analyses utilizing the KSN method were performed on PIBs produced in the presence of *n*-Bu_4NCl, at each polymerization temperature. Each sample possessed a relatively uniform distribution of chromophores throughout, with the KSN plots displaying near-linear relationships with slopes and intercepts of approximately unity and zero, respectively (Table 3). Slight dislocations in the KSN plots were apparent, however, within relatively narrow ranges of elution volume on the low molecular weight side of the RI and UV chromatograms. For a representative sample, Figure 7 shows GPC traces and KSN plot in which the dislocation has been bracketed by vertical lines. In general, the observed dislocations separate the KSN plots into two separate linear regions with similar slopes but different *y*-intercepts. The origin of the observed dislocations and *y*-intercept variations within the KSN plot is an inhomogeneity of chromophores within the distribution of molecular weights, the cause of which must logically be due to either a small fraction of proton-initiated chains (UV-invisible) or chains that possess more than one aromatic moiety per molecule. The only mechanism envisioned to produce multiple chromophores within a single macromolecule is chain coupling; however, previous results within our laboratory have shown clear chromatographic separation of chain-coupled material from the main distribution. Since coupled chains are not evident in the GPC chromatogram, coupling can be eliminated as a plausible explanation for the anomalous KSN plots for the *n*-Bu_4NCl-mediated systems. Since *n*-Bu_4NCl cannot scavenge protic impurities, the materials produced in its presence should contain a fraction, albeit very small, of proton-initiated chains; therefore, we propose that the KSN plot dislocations observed for *n*-Bu_4NCl-mediated systems are due to proton initiation. Because the ratio [*t*-Bu-*m*-DCC]$_0$/[H^+] is very large under these conditions, the overall contribution of protic initiation is extremely small; moreover, the efficiency and rate of protic initiation are not as great as that of the purposefully added cumyl-type initiator. Polymerizations conducted in the absence of *t*-Bu-*m*-DCC showed that protic initiation is not sup-

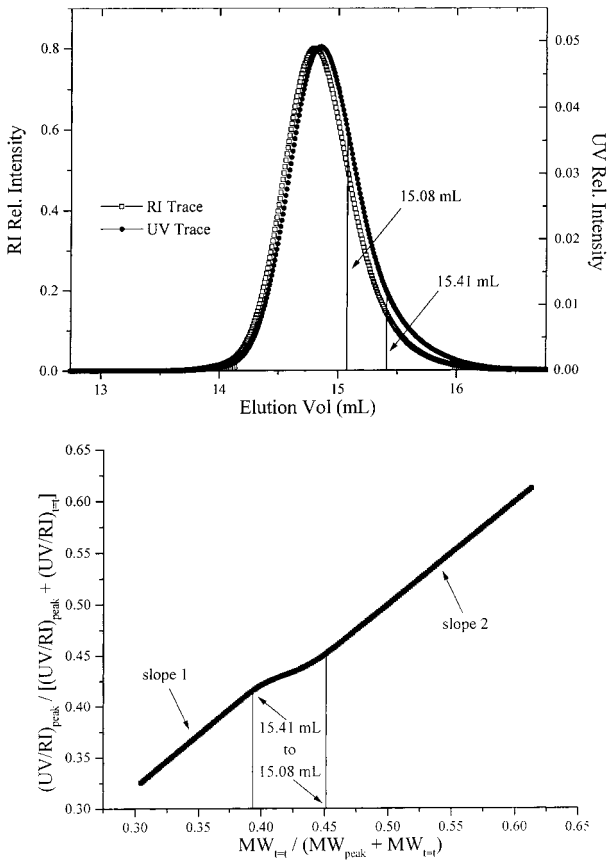

Figure 7. Top: RI and UV GPC traces of PIB produced at −80 °C. $[IB]_0 = 1.0$ M; $[t\text{-Bu-}m\text{-DCC}]_0 = 1.19 \times 10^{-2}$ M; $[TiCl_4]_{nom} = 0.12$ M; $[n\text{-Bu}_4NCl] = 5.4 \times 10^{-3}$ M; 60/40 Hex/MeCl cosolvents (v/v). Bottom: Kennedy−Smith−Nagy analysis of GPC traces, excluding fractions at very high and very low elution volumes (shaded areas in top figure).

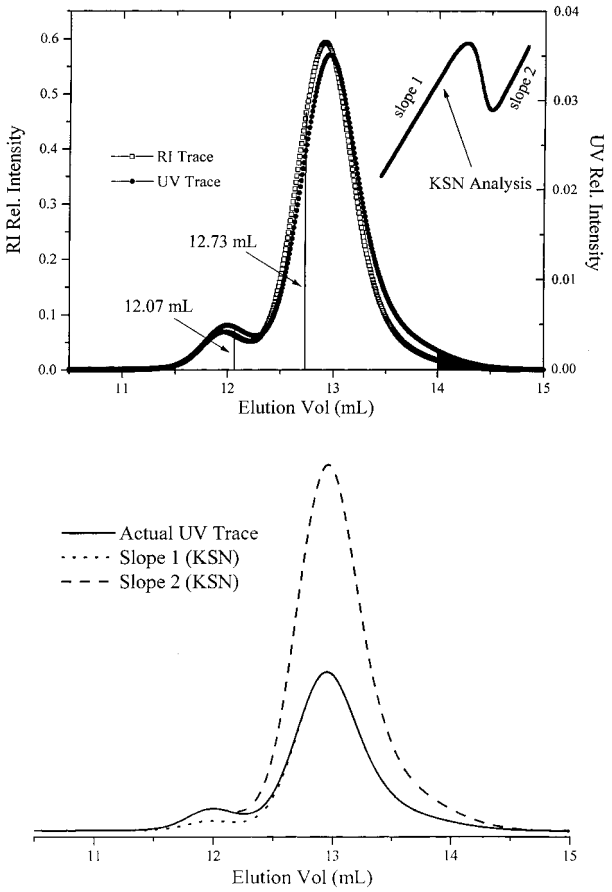

Figure 8. Top: RI and UV GPC traces with KSN plot (inset) of PIB ($M_n = 4900$ g/mol, PDI = 1.15) containing 6.3 wt % chain-coupled material. Bottom: theoretical UV traces fabricated from linear regions of KSN plot.

pressed by the use of n-Bu_4NCl at −80 °C; however, these polymerizations displayed slow initiation and required nearly 13 times longer to produce similar IB conversions. It is highly unlikely that the small fraction of UV-invisible chains could have originated from chain transfer to monomer since its presence would have caused characteristic downward curvature in M_n vs conversion plots, which was not observed at any polymerization temperature studied.

To confirm our interpretation of the KSN analyses, investigations were performed on well-characterized PIBs containing varying fractions of chain coupled and UV-invisible chains. To this end, both RI and UV GPC traces were obtained for two separate materials: first, a *t*-Bu-*m*-DCC-initiated PIB (4900 g/mol) containing a known chain-coupled mass fraction of 6.3%; second, a blend of two monodisperse PIBs (both 2000 g/mol), with one containing the *t*-Bu-*m*-DCC moiety and the other initiated with 2-chloro-2,4,4-trimethylpentane (TMPCl) (UV-transparent). Both analyses revealed dramatic dislocations in the KSN plots, with large variations between initial and terminal intercepts. RI and UV traces, along with the corresponding KSN plot, for the PIB containing a fraction of chain-coupled material are displayed in Figure 8. The inflection points in the KSN plot represent end points of the range of elution volumes over which the distributions of monomeric and dimeric chains overlap. Over this range both types of chains are eluting simultaneously, and the average number of UV chromophores per chain in each elution slice is changing from two to one (moving from low to high elution volume). Strikingly, the inhomogeneity within the chromophore distribution leads to a distinct change in intercepts within the KSN plot, not an appreciable modification of the slopes after inflection. Using either linear region of the KSN plot, theoretical UV traces may be fabricated (Figure 8, bottom), which represent the chromatographic UV-detector responses needed to accurately match the RI-detector response of PIB containing uniformly either one or two chromophores per chain, thus producing linear KSN relationships throughout the entire polymer sample. The theoretical UV trace corresponding to one chromophore per PIB chain shows a diminished response within the region of the chain-coupled fraction (dotted trace). Likewise, assuming two chromophores per chain causes intensification of the response within the lower molecular weight fraction (dashed trace). These theoretical traces accord well with expectation given the known chromophoric inhomogeneity within this sample. KSN analysis of the PIB blend produced a plot with very similar characteristics to the one obtained with the chain-coupled PIB sample; however, an even greater dislocation was observed between the two separate linear regions. The linear region corresponding to low elution volume (known to be UV-active from preliminary GPC analysis of the individual PIBs) was used to fabricate a theoretical UV trace that would result if all chains contained one chromophore (Figure 9). Qualitatively, the fabricated UV trace accurately coincides with the RI response, thus giving the appearance of chromatogram sets obtained from monodisperse, UV-active PIBs analyzed within this study.

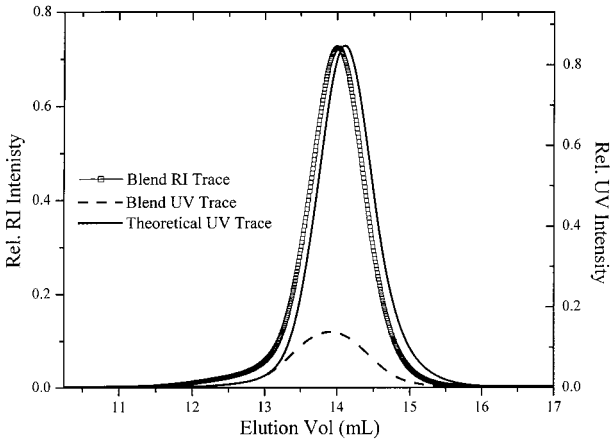

Figure 9. RI (open squares) and UV (dashed line) GPC traces of a binary blend of UV-transparent (M_n = 2000 g/mol, TMPCl initiated) PIB and UV-active (M_n = 2000 g/mol, *t*-Bu-*m*-DCC initiated) PIB, and theoretical UV trace (solid line) required to match RI GPC traces assuming one chromophore per PIB chain.

Therefore, the characteristic dislocations detected within the KSN analysis may originate from UV-transparent macromolecules eluting at relatively high elution volumes (protic initiation), polymer chains containing multiple UV-active chromophores eluting at relatively low elution volumes (chain coupling), or a combination of both. Elucidation of the predominant mechanism responsible for nonlinearity, however, may be intuitively deduced by examination of theoretical UV chromatograms constructed from each linear region within the KSN plot. The methodology described above was used to analyze RI traces obtained for all PIBs produced in the presence of *n*-Bu_4NCl. Preliminary evaluations of KSN plots showed no deviations between theoretical and actual UV traces, except that the latter were slightly lower in intensity at higher elution volumes. These results indicate the presence of an extremely small fraction of proton-initiated chains that are of significantly lower-than-targeted molecular weight (≈1400 g/mol).

The effect of the *n*-Bu_4NCl concentration on the rate of polymerization was determined by measuring the apparent rate constant at −70 °C using various *n*-Bu_4NCl concentrations, while holding the concentration of IB, *t*-Bu-*m*-DCC, and $TiCl_4$ constant at 1.0, 1.19×10^{-2}, and 0.12 M, respectively, within a Hex/MeCl (60/40 v/v) cosolvent mixture. Figure 10 shows the first-order kinetic plots for the various *n*-Bu_4NCl concentrations studied, with the individual k_{app}'s given in Table 2. The polymerization rate was independent of [*n*-Bu_4NCl], and the resultant PIBs possessed the targeted molecular weight and very low polydispersities (PDI < 1.1). However, the solubility of *n*-Bu_4NCl within these polymerization mixtures is limited, with even the lowest [*n*-Bu_4NCl] providing a heterogeneous slurry before and after the addition of $TiCl_4$. In addition, IR spectra taken before the addition of $TiCl_4$ displayed no distinct absorbance bands within the spectral limits of our instrument that could be attributed to soluble *n*-Bu_4NCl. Since each of the polymerization systems that utilized *n*-Bu_4NCl exhibited linearity in both the first-order kinetic plots and M_n vs IB conversion plots, a finite quantity of solvated *n*-Bu_4NCl must be available with the introduction of $TiCl_4$ to produce a sufficient concentration of the common anion, $Ti_2Cl_9^-$.

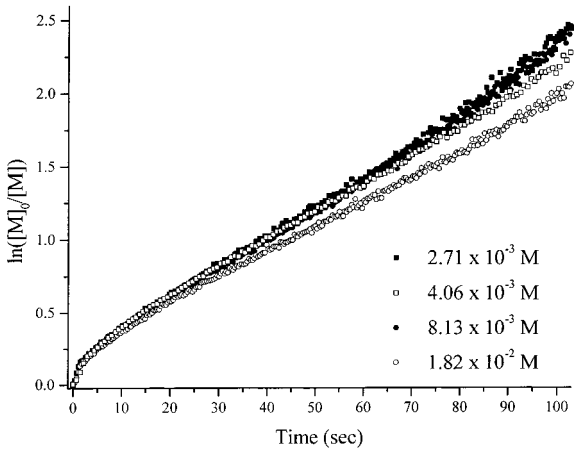

Figure 10. Effect of [*n*-Bu_4NCl] on the rate of polymerization of IB at −70 °C. $[IB]_0$ = 1.0 M; [*t*-Bu-*m*-DCC]$_0$ = 1.19×10^{-2} M; $[TiCl_4]_{nom}$ = 0.12 M; 60/40 Hex/MeCl cosolvents (v/v).

Effect of Temperature and Common Ion Salt/Lewis Base Combinations on IB Polymerizations. We hypothesized that a common ion salt/Lewis base combination might synergistically enhance polymerization rate and molecular weight control in IB polymerizations. To test this idea, two series of polymerizations were carried out at −40, −60, and −80 °C, with each system utilizing a combination of *n*-Bu_4NCl and DMP or *n*-Bu_4NCl and D*t*BP. Both series employed [*n*-Bu_4NCl] = 5.4×10^{-3} M and [DMP] (or [D*t*BP]) = 2.5×10^{-3} M, while the concentrations of IB, *t*-Bu-*m*-DCC, and $TiCl_4$ were held constant at 1.0, 1.19×10^{-2}, and 0.12 M, respectively, within a Hex/MeCl (60/40 v/v) cosolvent mixture. The semilogarithmic first-order kinetic plots were virtually identical to those shown earlier in Figure 1, except that the rates of polymerization were consistently slightly lower when the combination of additives was used; the individual k_{app}'s are listed in Table 2. When *n*-Bu_4NCl was utilized in combination with either of the Lewis base additives, the resultant kinetic behavior mimicked that of a system employing the corresponding Lewis base in isolation. In contrast, however, the high molecular weight leading shoulder observed at early IB conversions in the Lewis base-mediated polymerizations (e.g., Figure 4) was substantially reduced, which is very similar to the behavior of polymerizations containing *n*-Bu_4NCl only. Correspondingly, KSN analysis of RI and UV GPC traces obtained from polymerizations utilizing *n*-Bu_4NCl/Lewis base combinations revealed completely linear relationships with slopes of unity possessing zero *y*-intercepts.

All polymerizations containing Lewis bases and/or common ion salts displayed a strong increase in k_{app} with decreasing polymerization temperature (Table 2), indicating a negative apparent activation energy, E_{act}, for IB polymerizations under these conditions. This phenomenon has been often observed for quasiliving carbocationic systems, with a value of −8.5 kcal/mol having been earlier reported by Storey et al.,[22] and confirmed by others[37] for IB polymerizations co-initiated with $TiCl_4$ in 60/40 hexane/MeCl cosolvents. To obtain E_{act} values from the kinetic data herein, semilogarithmic plots of ln(k_{app}) vs reciprocal temperature were constructed (Supporting Information, Figure F). Although the relationships were linear, and the apparent activation energies were approximately equal for all three

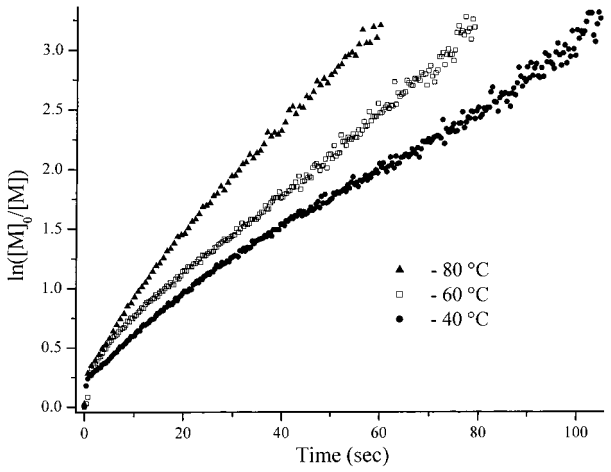

Figure 11. First-order kinetic plots for IB control polymerizations (absence of additives) at various temperatures. $[IB]_0 = 1.0$ M; $[t\text{-Bu-}m\text{-DCC}]_0 = 1.19 \times 10^{-2}$ M; $[TiCl_4]_{nom} = 0.12$ M; 60/40 Hex/MeCl cosolvents (v/v).

polymerization additives, the observed values of −(5.3−5.5) kcal/mol (Table 2) are considerably higher than the previously reported value of −8.5 kcal/mol. The difference between this and the earlier study is the much greater rate of polymerization and the vastly larger polymerization exotherm that results. The systems herein produced low molecular weight PIB (≈5000 g/mol) in reaction times of less than 60 s for the lowest temperature and the higher $[TiCl_4]_{nom}$. Under these extreme conditions, the reactor temperature would rise by as much as 15 °C, and thermal reequilibration would not occur until several half-lives after essentially complete monomer consumption. By virtue of the characteristic negative apparent activation energy that characterizes these quasiliving systems, the polymerization exotherms were more severe at lower temperatures, causing increases in actual reactor temperature, and concomitant retardations in rate, which were likewise more severe at lower temperatures. This effect produced a higher apparent E_{act}. Subsequent evaluations of the same kinetic data employing the actual average reactor temperature (recorded using the platinum resistance thermometer) instead of the nominal polymerization temperature produced linear Arrhenius relationships with slopes averaging −7.1 kcal/mol, more closely approximating the E_{act} value commonly reported for this system.

Effect of Temperature on "Conventional" IB Polymerizations. To gain further insight into the mechanistic differences between conventional (nonliving) and quasiliving carbocationic polymerizations of IB, control experiments were performed in the absence of any proton trap, nucleophile, or common-ion salt additive. The effect of temperature on the rate of conventional IB polymerizations was investigated by measuring the kinetics for polymerizations at −40, −60, and −80 °C while holding concentrations of IB, *t*-Bu-*m*-DCC, and $TiCl_4$ constant at 1.0, 1.19×10^{-2}, and 0.12 M, respectively, within a Hex/MeCl (60/40 v/v) cosolvent mixture. The results are displayed as first-order kinetic plots in Figure 11; k_{app}'s were extracted from the linear portions of the curves (times greater than about 25−30 s) and are listed in Table 2. Two features of the curves are striking. First, regardless of temperature, about 22% of the monomer is consumed almost instantaneously, after which a relatively more controlled polymerization ensues. Second, although these reactions are characterized by an apparent negative dependence of polymerization rate on reaction temperature, unlike the systems mediated by additives, the dependence is not nearly as strong. For example, the polymerization conducted at −80 °C was only 1.8 times faster than the one at −40 °C. In contrast, the rate increased by about a factor of 10 over the same temperature range, under otherwise identical conditions in the presence of an additive. The characteristic negative apparent E_{act} noted for quasiliving carbocationic polymerizations has been attributed to the ionization equilibrium between active and reversibly terminated (dormant) chains.[22,30,37] Modest increases in reaction temperature markedly reduce the overall rate because of a reduction in the instantaneous concentration of active propagating centers. Undoubtedly, this ionization equilibrium operates whether a Lewis base or other additive is present or not. Comparison of the apparent rate constants in Table 2 shows that the rate at −80 °C is relatively unaffected by the presence or absence of additives. However, the rate at −40 °C is significantly higher in the absence of an additive, and it is this effect that causes the relative insensitivity toward temperature of the conventional polymerizations. According to literature reports, the dramatically higher rate in the absence of an Lewis base is due to uncontrolled initiation by protic impurities.[3,7,13,50]

GPC analysis of the conventional IB polymerizations (Figure 12) revealed bimodal molecular weight distributions at all three reaction temperatures; furthermore, the mass fraction of high molecular weight material diminished as reaction temperature was lowered. Peak deconvolution of the RI GPC traces revealed that the high MW distributions comprised approximately 90, 64, and 23 wt % of the sample for polymerization temperatures of −40, −60, and −80 °C, respectively. On the basis of literature reports,[3,7,13,50] we initially assumed that the high molar mass distribution resulted from fast, uncontrolled protic initiation; however, the results of two different analyses showed this to be incorrect. First, the overall number-average molecular weight (both modes of the distribution combined) was equal to the target (number-average DP = 84) for all three temperatures. Second, the KSN plot (Figure 12) constructed from the RI and UV traces of the −40 °C PIB was linear with a slope of unity that passed through the origin. These results verified that all chains within both modes of the distribution possess the same number of UV-active initiator fragments. Further analysis of GPC traces produced at lower polymerization temperatures gave similar results; however, there were slight dislocations within the KSN plots at −60 and −80 °C (Figure 12 and Table 3). These departures from linearity were of greater magnitude than those seen in the *n*-Bu_4NCl-mediated IB polymerizations under similar conditions but were much less severe than those observed with either the purposefully chain-coupled or UV active/transparent PIB blend described earlier. The methodology outlined earlier was used to develop theoretical UV traces that would fulfill the condition that every chain in the sample possesses the same number of chromophores (i.e., one per chain). Figure 13 shows the fabricated UV traces for −60 °C (top set) and −80 °C (bottom set). The results were the same at both temperatures; to ensure one chromophore per chain required suppression of the higher molar mass fraction (dotted trace) or enhancement of the lower fraction

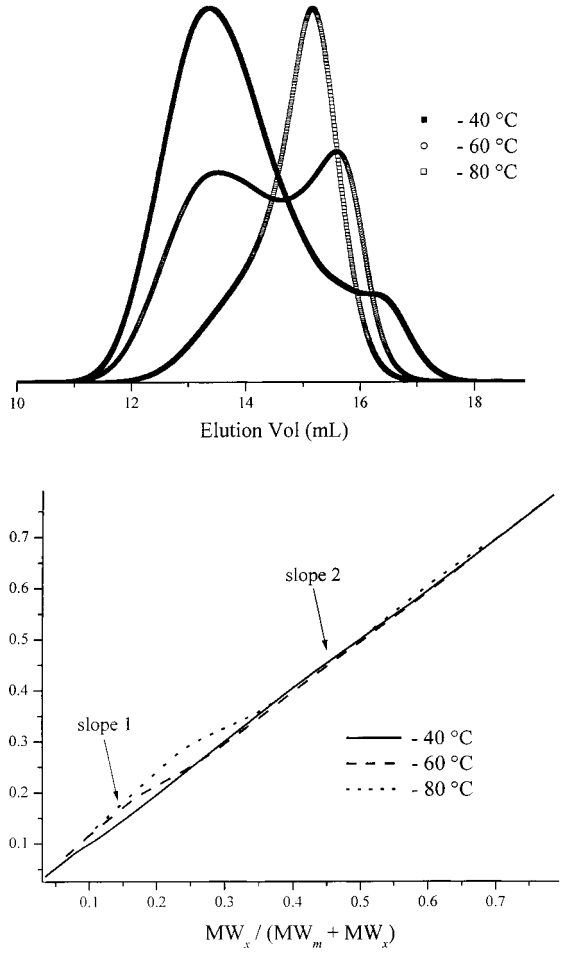

Figure 12. Top: RI GPC traces of PIB produced at various temperatures under conventional conditions (no additives). $[IB]_0 = 1.0$ M; $[t\text{-Bu-}m\text{-DCC}]_0 = 1.19 \times 10^{-2}$ M; $[TiCl_4]_{nom} = 0.12$ M; 60/40 Hex/MeCl cosolvents (v/v). Bottom: Kennedy–Smith–Nagy analysis of GPC traces of top figure.

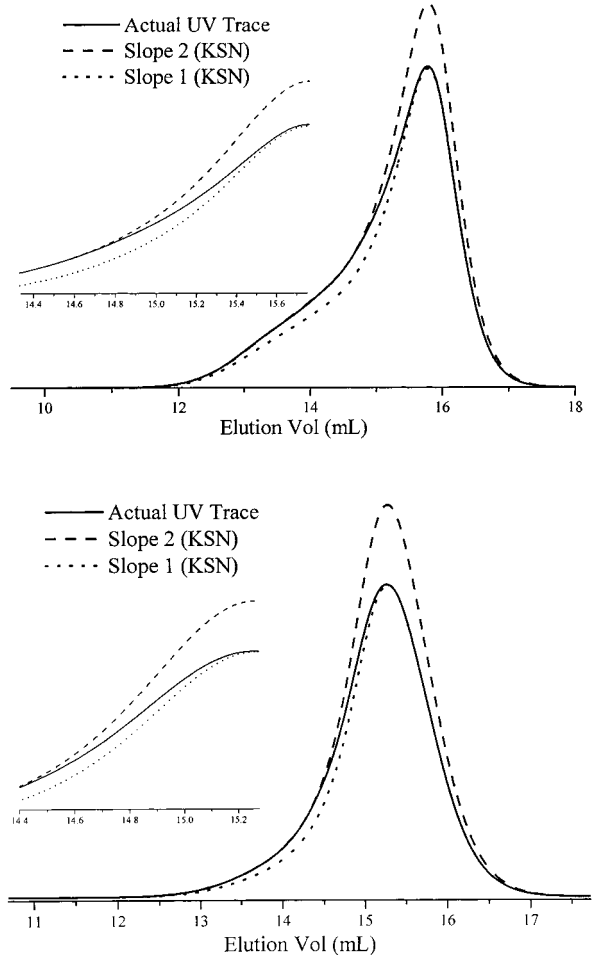

Figure 13. Theoretical UV traces fabricated from KSN analysis in Figure 12 of nonmediated IB polymerizations at −60 °C (top set) and −80 °C (bottom set).

(dashed trace). Qualitative interpretation of these data is ambiguous, since chain–chain coupling and/or protic initiation may induce similar inflections within KSN plots. It is certain, however, that the high molecular weight fraction is not a consequence of uncontrolled protic initiation. In fact, protic initiation should produce low molecular weight chains, since it is slower than *t*-Bu-*m*-DCC initiation, and consequently, protic-initiated chains would begin to propagate only after much of the monomer had been consumed.

Role of Additives in Quasiliving Carbocationic Polymerization. First-order kinetic evaluations of IB polymerizations conducted in the absence of a Lewis base or common ion salt resulted in extremely fast polymerization rates at higher (e.g., −40 °C) temperatures where quasiliving polymerizations (i.e., those carried out in the presence of an additive) are significantly decelerated. GPC analysis of the same reactions revealed bimodal distributions within both UV and RI traces (Figure 12). Quantitative KSN analysis showed that both modes of the distribution were composed of polymer molecules containing a residue from the purposefully added aromatic initiator and that the amount of protic initiation and/or chain coupling was negligible, particularly at the highest temperature studied (−40 °C). Bimodality observed in the absence of an additive suggests that propagation proceeds via two distinctly different active centers. Moreover, the enhanced polymerization rates imply a greater total concentration of active centers, i.e., that formation of the second type of species does not significantly perturb the equilibrium concentration of the first. We propose that the additional active species in the absence of an additive, responsible for the higher molar mass fraction, is the free carbocation, P^+, resulting from dissociation of an ion pair. We reject the explanation that the more active species represents chain ends that have yet to become associated with an electron donor:$TiCl_4$ complex.[3,7−10] The reasons for this are twofold: first, several authors have argued that a D*t*BP:$TiCl_4$ complex does not exist;[13,14,44] second, polymerization rates are significantly reduced, and the molecular weight distribution becomes monomodal and narrow upon the addition of the common ion salt, *n*-Bu_4NCl. Clearly the tetravalent ammonium ion is nonnucleophilic and cannot form a complex with Lewis acid. Assuming IB polymerizations mediated by *n*-Bu_4NCl are converted from "conventional" to quasiliving strictly due to the suppression of free ions via the production of the common anion $Ti_2Cl_9^-$, it stands to reason that Lewis bases must operate in a similar fashion. It is well established that externally added Lewis bases scavenge protic impurities;[13,50] the product(s) formed from such processes are onium salts, which in the presence of excess $TiCl_4$, possess the counteranion, $Ti_2Cl_9^-$. Formation of common anions is shown below for the case of water (B = a Lewis base such as DMP).

$$B + H_2O{\cdot}TiCl_4 \rightleftharpoons BH^+TiCl_4OH^- \quad (4)$$

$$BH^+TiCl_4OH^- + TiCl_4 \rightleftharpoons BH^+Ti_2Cl_8OH^- \quad (5)$$

$$BH^+Ti_2Cl_8OH^- + TiCl_4 \rightleftharpoons BH^+Ti_2Cl_9^- + TiCl_3OH \quad (6)$$

Thus, we postulate that Lewis bases and *n*-Bu_4NCl confer "livingness" in the same manner, i.e., through the formation of common anions that suppress propagation via free ions. This hypothesis is the same as the one put forth by Storey and Maggio to explain the absence of free carbocations within BCl_3-*co*-initiated IB polymerizations in CH_3Cl.[51] In the case of $TiCl_4$, however, the proton scavenging function of Lewis bases also prevents protic initiation, which becomes increasingly important at low concentrations of purposefully added initiator and at low temperatures. The broad leading shoulder observed in GPC traces of Lewis base-mediated polymerizations at low conversion is likely attributed to a transient initial population of free ions that form before the formation of common anions, via proton scavenging, has had time to take place. Apparently, *n*-Bu_4NCl is able to from $Ti_2Cl_9^-$ anions more rapidly, thus reducing the amount of monomer consumed by free ions prior to their complete suppression.

Two experiments were conducted to add support to the hypothesis that Lewis bases confer "livingness" primarily through suppression of free-ion propagation. One involved the addition of preformed pyridinium salt; the other involved promotion of ion pair dissociation through chain-end dilution. To model common anion formation via the reaction of adventitious proton sources with $TiCl_4$ and Lewis base, an investigation was performed using pyridine hydrochloride (Pyr-HCl) as the polymerization additive. A pyridine-based salt was chosen for its ready availability and due to the fact that pyridine-mediated IB polymerizations under conditions similar to those described in this report display quasiliving characteristics.[22] IB polymerizations were carried out at −70 °C, with the concentrations of Pyr-HCl, *t*-Bu-*m*-DCC, IB, and $TiCl_4$ being 4.3×10^{-3}, 1.19×10^{-2}, 1.0, and 0.12 M, respectively, within a Hex/MeCl (60/40 v/v) cosolvent mixture. Because of the limited solubility of Pyr-HCl within the reaction medium, two experimental procedures were used to investigate its effect on the rate of polymerization. In the first method, all of the reaction components were mixed thoroughly at −70 °C, after which the polymerization was co-initiated by $TiCl_4$; the second method employed an initiating solution of MeCl, $TiCl_4$, and Pyr-HCl (keeping component concentrations the same as in the first method) that was preformed at −70 °C and then added to the reaction vessel to commence polymerization. The resulting first-order kinetic plots are shown in Figure 14, with the k_{app}'s given in Table 2. Polymerizations utilizing neat $TiCl_4$ were extremely fast, reaching near-complete IB conversion in less than 50 s; furthermore, a large heat of reaction was generated upon co-initiator addition, inducing temperature increases of approximately 15 °C. GPC analysis of the resultant PIB revealed a bimodal MWD identical to the ones obtained from the conventional systems described earlier. Visual inspection of the reaction solution before $TiCl_4$ addition indicated poor Pyr-HCl solubility within the relatively nonpolar cosolvent system, with the FTIR analysis of the mixture supporting this observation; however, we

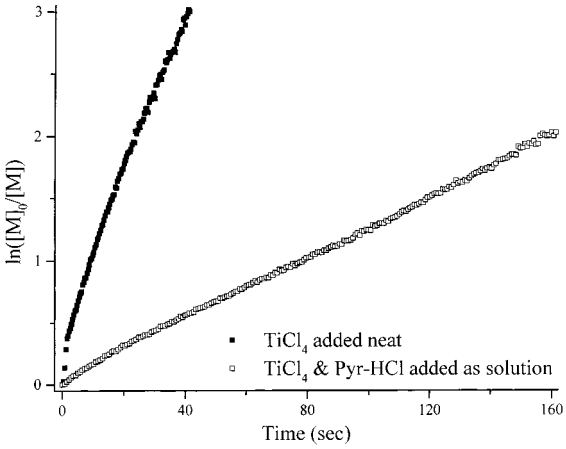

Figure 14. First-order kinetic plot for the Pyr-HCl-mediated polymerizations of IB at −70 °C. $[IB]_0 = 1.0$ M; $[t\text{-Bu-}m\text{-DCC}]_0 = 1.19 \times 10^{-2}$ M; $[TiCl_4]_{nom} = 0.24$ M; $[Pyr\text{-}HCl] = 4.3 \times 10^{-3}$ M; 60/40 Hex/MeCl cosolvents (v/v). Filled symbols, $TiCl_4$ added neat; open symbols, $TiCl_4$ and Pyr-HCl added as a premixed solution in MeCl.

expected its solubility to increase upon introducing $TiCl_4$. To discern whether the observed kinetic behavior were attributed to Pyr-HCl insolubility or its inherent reaction characteristics, polymerizations were co-initiated using the preformed solution described above. The co-initiator solution developed a large fraction of yellow-white precipitate with the introduction of Pyr-HCl to the $TiCl_4$/MeCl mixture; furthermore, this precipitate persisted after its charge into the IB-containing vessel, with the polymerization visually resembling the solutions of typical pyridine-mediated IB polymerizations. In this case, GPC analysis revealed a narrow, monomodal distribution of targeted average molecular weight. Assuming that the Pyr-HCl lacks the capability to scavenge protic impurities, the quasiliving behavior observed in the second polymerization system must be attributed to formation of the common ion salt, $PyrH^+Ti_2Cl_9^-$. The extremely high polymerization rate and bimodal molecular weight distribution obtained by the first method confirm two important assumptions. First, in the presence of monomer, the solubilization of Pyr-HCl upon the addition of $TiCl_4$ is a sluggish process and does not provide common ions to the system quickly enough; second, IB propagation within these "nonmediated" systems occurs through a combination of separate, yet distinct, active chain carriers.

Polymerizations in which propagation occurs via a combination of both paired and unpaired ions typically yield an increase in $k_{app}/[I]_0$ with decreasing $[I]_0$, as has been reported for living anionic polymerizations in polar solvents.[52,53] Similar investigations have been performed on $TiCl_4$-*co*-initiated IB polymerizations in the presence of Lewis bases, with results suggesting that only ion-paired species participate as chain carriers.[22,23] To further corroborate the hypothesis that conventional IB polymerizations are indeed characterized by free ion propagation, a series of IB polymerizations were conducted under similar conditions to those of the polymerizations described above; however, the $[t\text{-Bu-}m\text{-DCC}]_0$ was continually reduced to induce ion-pair dissociation through chain-end dilution. The experiments were carried out at −70 °C at four different $[t\text{-Bu-}m\text{-DCC}]_0$, in both the presence and absence of either DMP, D*t*BP, or *n*-Bu_4NCl, with the results given in Table 4. Minor variations in the $k_{app}/[t\text{-Bu-}m\text{-DCC}]_0$

Table 4. Effect of Chain-End Dilution on the k_{app}/[*t*-Bu-*m*-DCC]$_0$ Values for Quasiliving and Conventional (No Additive) Isobutylene Polymerizations[a]

additive	[*t*-Bu-*m*-DCC]$_0$ × 10^4 M	k_{app}/[*t*-Bu-*m*-DCC]$_0$ (L mol^{-1} s^{-1})
DMP	9.62	2.63
	14.56	2.39
	34.08	2.06
	66.75	2.18
D*t*BP	6.51	1.78
	12.71	1.86
	37.31	1.68
	65.44	1.71
n-Bu$_4$NCl	12.94	1.47
	19.84	2.10
	34.81	1.85
	64.41	1.72
no additive	6.17	5.80
	13.7	4.05
	36.31	3.02
	65.75	2.12

[a] Reaction conditions: [IB]$_0$ = 1.0 M; [*n*-Bu$_4$NCl] = 5.4 × 10^{-3} M; [DMP] (or [D*t*BP]) = 2.5 × 10^{-3} M; [TiCl$_4$]$_{nom}$ = 0.12 M; 60/40 Hex/MeCl cosolvents (v/v); temp = −70 °C.

values were noted for IB polymerizations employing either Lewis base or *n*-Bu$_4$NCl; however, conventional polymerizations demonstrated much larger increases in k_{app}/[*t*-Bu-*m*-DCC]$_0$ values with decreasing concentrations of *t*-Bu-*m*-DCC, signifying that propagation proceeds in part via a fraction of free carbocations. When examining the quasiliving IB polymerizations performed at −70 °C using [*t*-Bu-*m*-DCC]$_0$ = 1.19 × 10^{-3} M (Table 2), however, the k_{app}/[*t*-Bu-*m*-DCC]$_0$ values are much lower in all cases. This is caused by poor thermal control in these fast polymerizations. Since this chain-end concentration is relatively high, the resulting large reaction exotherm causes the actual temperature of the reactor contents to be higher than the nominal temperature of the polymerization. Thus, the k_{app}/[*t*-Bu-*m*-DCC]$_0$ values at this initiator concentration are depressed. Because of this, the dilution experiments in Table 4 were designed at low [*t*-Bu-*m*-DCC]$_0$ to avoid large exotherms and resulting poor thermal control.

Although it seems certain that the bimodal MWDs observed for nonmediated IB polymerizations are a result of propagation through a combination of paired and unpaired ions, certain incongruities remain to be explained. One concerns an issue discussed earlier by Kazsas, Puskas, and Litt,[23] namely, that the lifetime of a free cation is simply too long and propagation is too fast, to be consistent with the low degrees of polymerizations observed. Another is the fact that, in the absence of a common ion source (i.e., when [P$^+$] = [Ti$_2$Cl$_9^-$]), the extremely low overall concentration of carbocations (≈10^{-12} mol/L based on the rate constants of Roth and Mayr[27] and Faust et al.[28]) would dictate that the majority of ionized chains exist as free, dissociated ions. To restate the argument of Puskas et al.,[23] we will assume that essentially all of the propagating centers in the conventional IB polymerizations are in the form of free ions. (This does not appear to be true, particularly at −80 °C, but represents a limiting case.) From the first-order plot for −80 °C (Figure 11), we obtain an apparent rate constant, $k_{app} = k_p[P^+] = 4.7 \times 10^{-2}$ s^{-1}. Using a value of $k_p = 7 \times 10^8$ L mol^{-1}s^{-1} measured by Faust et al. for ion pair propagation[28] and assuming that paired and unpaired ions have similar reactivities, we obtain [P$^+$] = 7 × 10^{-11} mol/L. We can assign the shortest possible lifetime to a free carbocation by assuming that the rate of reassociation of cation and anion is diffusion-controlled. The average lifetime of a free carbocation, τ, is given by

$$\tau = \frac{[P^+]}{k_c[P^+][Ti_2Cl_9^-]} = \frac{1}{k_c[Ti_2Cl_9^-]} \qquad (7)$$

where k_c is the rate constant for ion-pair association, liberally approximated as 10^{10} L mol^{-1} s^{-1}. In the absence of a source of common ions, [P$^+$] = [Ti$_2$Cl$_9^-$], and τ under these conditions may be calculated according to eq 8.

$$\tau = \frac{1}{k_c[P^+]} = 1.5 \text{ s} \qquad (8)$$

We next calculate the kinetic chain length associated with such a lifetime (at [M] = 1 mol/L):

$$DP = 2k_p[M]\tau = 2 \times 10^9 \qquad (9)$$

where the number-average degree of polymerization, DP, is twice the kinetic chain length for a difunctional initiator in the absence of chain transfer. KSN analysis of the GPC chromatogram for the conventional polymerization at −80 °C revealed that, at most, only minor amounts of chain transfer to monomer could have occurred, which is further supported by the close agreement between the actual and targeted molecular weight; thus, chain transfer to monomer can be eliminated as an important reaction, and the kinetic chain length and DP/2 should be approximately equal. Clearly they are not; the number-average DP for the high molecular weight fraction of the −80 °C conventional polymerization was 155, almost 7 orders of magnitude smaller than predicted by eq 9. Although the assumption of 100% dissociation made in the above exercise is inaccurate, a more realistic approach utilizing a lower [P$^+$] and a combination of active propagation centers (i.e., paired and unpaired ions) would yield a longer lifetime for free, unpaired ions and thus even larger theoretical DP values for the high molecular weight fraction.

The great discrepancy between the calculated kinetic chain length and the observed DP for free ions, and the fact that essentially all molecules have the expected structure (i.e., a headgroup consisting of the aromatic initiator fragment), suggest (1) the presence of adventitious common anions, which could dramatically shorten the effective lifetime of free carbocations (eq 7) and would originate via proton scavenging by basic impurities within the system, in the presence of Lewis acid, and/or (2) chain transfer to dormant, *tert*-chloride-terminated chain ends, which would distribute the kinetic chain length of a free ion over many chains via an inifer-type mechanism.[47,54,55] The latter transfer reaction, characterized by the rate constant k_{tr}, is shown in Figure 15. We may now examine each of these possibilities in turn. The case for an adventitious common ion source is strong. The equilibrium constant for ion-pair dissociation, K_D (Figure 15), is estimated to be ≈10^{-7} mol/L.[56] If the total concentration of carbocations, [P$^+$,Ti$_2$Cl$_9^-$] + [P$^+$] = 7 × 10^{-11} mol/L, then >99.9% should be dissociated. Even if K_D were as low as 10^{-9} mol/L, >94.6% should be dissociated. However, the high molecular weight fraction in the −80 °C GPC trace in Figure 12 only represents about 10 mol % of the total, suggesting that dissociation is strongly de-

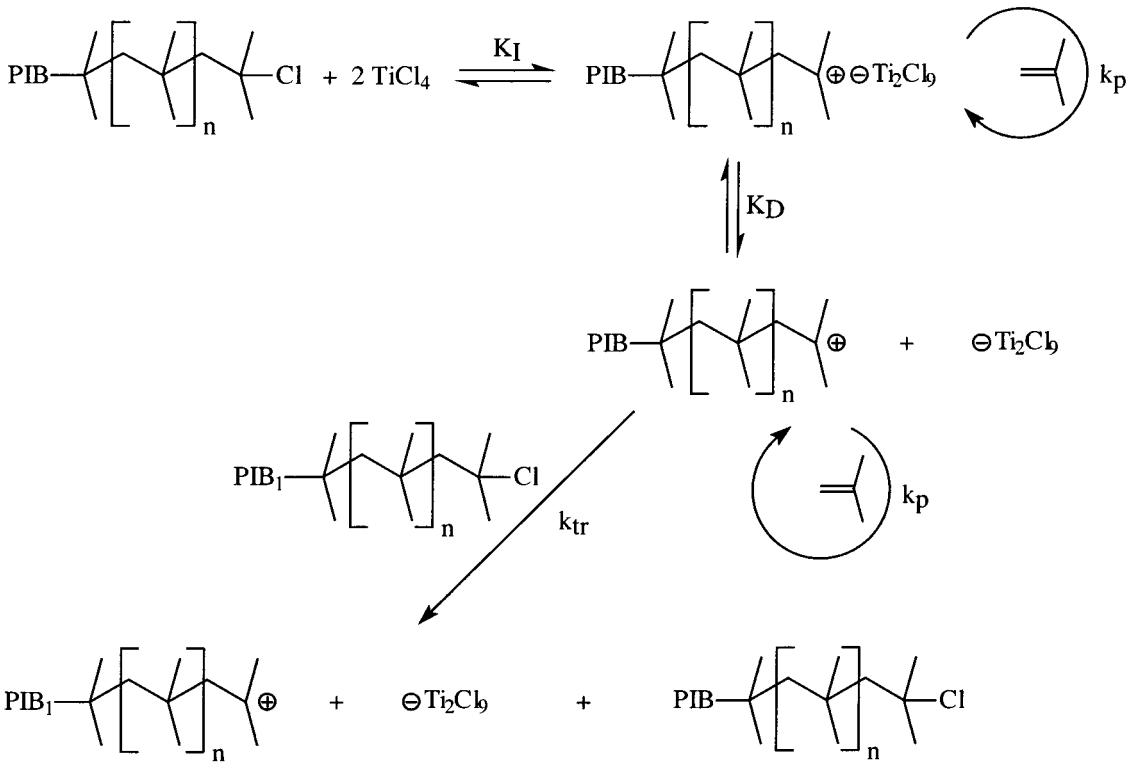

Figure 15. Proposed elementary reactions in the conventional carbocationic polymerization (no additives) of isobutylene.

pressed. For $K_D = 10^{-7}$ mol/L, a common ion concentration of $\approx 10^{-6}$ mol/L would be sufficient to reduce $[P^+]$ to within the necessary range suggested by the GPC results. This concentration of Lewis base impurity could be present and remain undetected in the system. Equations 7 and 9 predict, however, that the concentration of adventitious common ions would have to be on the order of $10^{-4}-10^{-3}$ mol/L to reduce the free carbocation lifetime sufficiently to produce kinetic chain lengths on the order of the observed DP; it is doubtful that proton scavenging impurities could be present at this high concentration. As will become clear, adventitious common ions are undoubtedly present and important in depressing free ion participation in propagation, but their presence is inadequate as a sole explanation for the observed molecular weight depression.

Let us now consider chain transfer to dormant, *tert*-chloride-terminated chain ends. This appears to be the only reasonable explanation for the observed DP of the high molecular weight distribution, and there is strong literature precedence for such reactions in carbocationic polymerization, e.g., the inifer mechanism proposed for BCl_3-*co*-initiated IB polymerizations using cumyl-type initiators.[54] If transfer to polymer occurs, and there is a source of common ions, eq 9 must be modified as follows:

$$\mathrm{DP} = \frac{2k_p[\mathrm{M}]}{k_{tr}[\mathrm{PIBCl}] + k_c[\mathrm{Ti_2Cl_9^-}]} \cong \frac{2k_p[\mathrm{M}]}{2k_{tr}[t\text{-Bu-}m\text{-DCC}]_0 + k_c[\mathrm{Ti_2Cl_9^-}]} \quad (10)$$

where k_{tr} represents the rate constant for free carbocation transfer to *tert*-chloride-terminated chains. We assume that the total concentration of active centers is small enough to use $[t\text{-Bu-}m\text{-DCC}]_0$ to represent the concentration of dormant chain ends. Equation 10 predicts that k_{tr}/k_p, the chain-transfer to polymer constant, must assume a value of about 0.3 (at an average value of [M] = 0.5 M) to obtain a number-average DP value that is similar to that found experimentally. This is within the range of values reported for the early inifer systems.[47,54] In the absence of a purposefully added source of common ions, the right-hand term in the denominator of eq 10 is negligible and does not affect the calculation. Even if a source of adventitious common ion were present to provide $[Ti_2Cl_9^-]$ as high as $10^{-5}-10^{-4}$ mol/L, chain transfer to polymer would still dominate. Equation 10 predicts that if such transfer events do indeed occur, their significance should be reduced, and the DP of the high molecular weight fraction increased, as $[t\text{-Bu-}m\text{-DCC}]_0$ is lowered. To demonstrate this, investigations were performed under identical conditions to the conventional −80 °C polymerization described earlier, but using $[t\text{-Bu-}m\text{-DCC}]_0 = 6.17 \times 10^{-4}$ mol/L. Figure 16 shows the RI and UV GPC traces of the PIB produced under these conditions. As predicted, the molecular weight of the high fraction (number-average DP = 1723) is considerably greater in this case compared to the earlier polymerization utilizing higher $[t\text{-Bu-}m\text{-DCC}]_0$. (The molecular weight ratio between high and low fractions is 6.7 in this case compared to approximately 2.4 for the earlier case.) If molecular weight were being controlled by adventitious common ions rather than chain transfer to polymer, eq 10 predicts that a reduction in $[t\text{-Bu-}m\text{-DCC}]_0$ should have little effect on molecular weight of the high fraction. Thus, chain transfer to dormant, *tert*-chloride-terminated chain ends emerges as the only reasonable explanation for the depression of the molecular weight of chains created through propagation of free carbocations. There remained a possibility, albeit very unlikely, that the chain transfer process described herein involves residual *t*-Bu-*m*-DCC that failed to initiate polymeri-

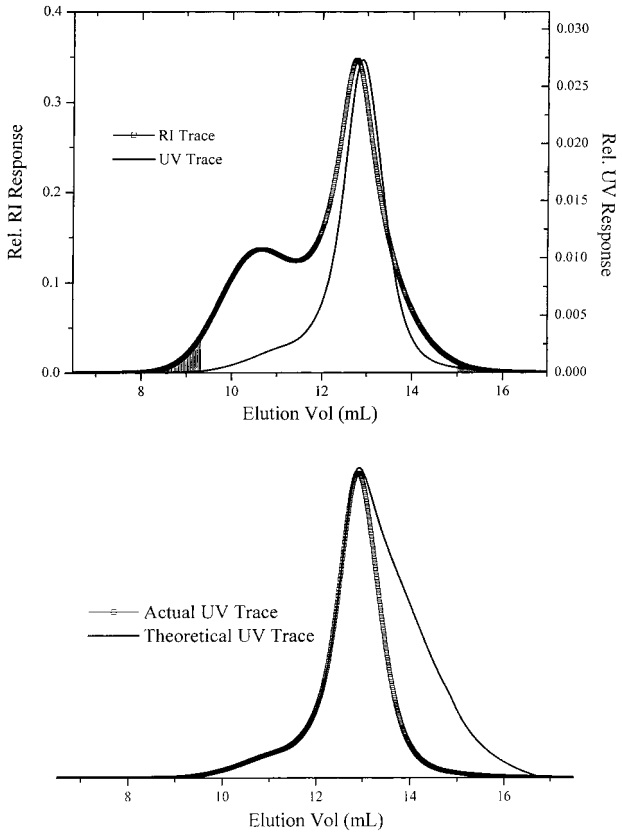

Figure 16. Top: RI and UV GPC traces of PIB produced at −80 °C. $[IB]_0 = 1.0$ M; $[t\text{-Bu-}m\text{-DCC}]_0 = 6.17 \times 10^{-4}$ M; $[TiCl_4]_{nom} = 0.12$ M; 60/40 Hex/MeCl cosolvents (v/v). Bottom: theoretical UV traces fabricated from linear regions of KSN plot (not shown).

zation and not dormant *tert*-chloride-terminated PIB chain ends. Additional polymerizations were performed using TMPCl under otherwise identical conditions as the −40 °C conventional system reported above using *t*-Bu-*m*-DCC. Typical of TMPCl-initiated IB polymerizations, the first-order kinetic plot (not shown) was void of an apparent *y*-intercept (no rapid monomer consumption event), due to the similar ionization equilibrium constants for TMP−Cl and *tert*-chloride PIB chain ends; however, the $k_{app} \approx 2.1 \times 10^{-2}$ s^{-1} was very similar to the $k_{app} \approx 2.6 \times 10^{-2}$ s^{-1} for the *t*-Bu-*m*-DCC-initiated conventional IB polymerizations. Further similarities were noted in the GPC evaluations, with TMPCl producing a bimodal MWD of targeted M_n analogous to the behavior seen with *t*-Bu-*m*-DCC.

The polymerization reaction of Figure 16 contains additional information concerning the occurrence of protic initiation. KSN analysis of the product exhibited a large dislocation within the high elution volume regime of the GPC trace; furthermore, a theoretical UV trace fabricated to compensate for the dislocation (bottom trace of Figure 16) suggests the presence of a fraction of UV-invisible chains located at higher elution volumes. We envision that protic initiation becomes more competitive at lower $[t\text{-Bu-}m\text{-DCC}]_0$, thus producing relatively larger mass fractions of UV-transparent macromolecules; furthermore, assuming that the initiating efficiency of both sources is similar, the molecular weights produced from protic initiation would be approximately half that of chains initiated by difunctional *t*-Bu-*m*-DCC.

Table 5. Estimated Values for $[P^+]$ and $[P^+,Ti_2Cl_9^-]$ in Isobutylene Polymerizations Conducted under Conventional Conditions[a]

temp (°C)	$[P^+]$ (mol/L)	$[P^+,Ti_2Cl_9^-]$ (mol/L)
−40	3.3×10^{-11}	3.7×10^{-12}
−60	3.0×10^{-11}	1.7×10^{-11}
−80	1.5×10^{-11}	5.2×10^{-11}

[a] Reaction conditions: $[IB]_0 = 1.0$ M; $[t\text{-Bu-}m\text{-DCC}]_0 = 1.19 \times 10^{-2}$ M; $[TiCl_4]_{nom} = 0.12$ M; 60/40 Hex/MeCl cosolvents (v/v).

A final intriguing feature of the nonmediated IB polymerizations is the decreasing contribution of free ions to propagation as temperature is lowered. From kinetics measurements, we know that the instantaneous concentration of active centers increases with decreases in polymerization temperature within quasiliving carbocationic processes.[22,30] This behavior is attributed to an equilibrium between dormant, covalent chain ends and active, ion-paired carbocations.[22,30,37] Assuming that a similar equilibrium exists between paired and unpaired ions, one might expect the mass fraction of the high molar mass distribution found within conventional polymerizations also to increase with decreasing polymerization temperatures. The ratio of the areas of the low and high molecular weight distributions in the RI GPC traces in Figure 12, obtained by deconvolution and integration, represents approximately the ratio of the concentrations of paired and unpaired ions at each temperature. The apparent rate constant obtained at each temperature, divided by the absolute rate constant for propagation, which for simplicity is assumed to be independent of temperature and the same for paired and unpaired ions (i.e., $k_p^+ = k_p^{\pm} = 7 \times 10^8$ L mol^{-1} s^{-1}), yields the total concentration of active species, $[P^+,Ti_2Cl_9^-] + [P^+]$. From this information, the quantities $[P^+]$ and $[P^+,Ti_2Cl_9^-]$ were estimated for each temperature, and the values are listed in Table 5. The paired-ion concentrations are very close to the corresponding values calculated for the D*t*BP-mediated polymerizations conducted under otherwise identical conditions; furthermore, calculation of an Arrhenius activation parameter for the paired-ion concentration yielded a value of −5.8 kcal/mol, which nearly exactly matches the values measured under quasiliving conditions. Thus, the paired ions in the conventional polymerization behave exactly like those in a quasilivng polymerization (i.e., in the presence of an additive) and, importantly, exhibit the expected behavior with regard to temperature. In contrast, the free ion concentration decreases with decreasing temperature, although the magnitude of change is not large (1.9 kcal/mol). This is the reason for the relative temperature insensitivity of the rate of the conventional polymerizations relative to the quasiliving polymerizations. The temperature dependence of the free ion concentration suggests that the ion-pair dissociation enthalpy may be positive, although only slightly so. The few literature reports that exist concerning the temperature dependence of ion-pair dissociation in carbocationic polymerization indicate that this process is generally slightly exothermic,[57] but in all cases the systems were studied in polar solvents, and we assume that solvation of the dissociated carbocation is the principal cause of the negative enthalpy. Thus, it is possible that in the largely nonpolar 60/40 hexane/MeCl medium, which should be poorly solvating, the dissociation enthalpy is positive. Even if the dissociation enthalpy were negative, a compelling alternative explanation for the observed behavior concerns adventi-

tious common ions, which are undoubtedly present in our system, produced through proton scavenging by trace amounts of basic impurities, in the presence of Lewis acid. It is conceivable that production and dissolution of these common ions are slightly more favorable at lower temperatures, thereby depressing the free-ion concentration.

Conclusions

The quasiliving polymerization of IB can be affected through the use of polymerization additives such as Lewis bases[1−3,8,9,13−22] and/or common ion salts.[15−24] In the past, rationalization of this controlled behavior has been system-specific, and the establishment of a unified theory explaining the origin of "livingness" has been prevented due to competing theories[8,11−13] regarding the mechanistic role of polymerization additives. It seems evident that a simple, universal theory treating the conversion between conventional and controlled systems should be applicable to all "living" carbocationic polymerizations. Using real-time ATR−FTIR spectroscopy, kinetics of fast IB polymerizations, producing relatively low molecular weight materials, have been examined. From the kinetic results, combined with detailed structural analysis of these low molecular weight materials, we hypothesize that conventional IB polymerizations (i.e., those conducted in the absence of an additive), under the conditions given in this report, are relatively free of chain transfer to monomer but are propagated via a combination of paired and unpaired ions. This causes poor synthetic control due to very fast rates and bimodal molecular weight distributions.

n-Bu_4NCl and other common ion salt precursors confer livingness through formation of the common anion, $Ti_2Cl_9^-$; this suppresses free ion propagation, reduces the rate of polymerization, and yields narrow PDI. Salts do not prevent protic initiation, however. Nucleophiles such as DMP and proton traps such as D*t*BP do scavenge protons and thus prevent protic initiation. This is an important feature for control of initiation, particularly for systems targeting high molecular weights, where the concentration of the intended initiator is low. We propose, however, that the products of proton scavenging, i.e., onium salts possessing common counteranions, are the principal contributors to quasiliving behavior. We suggest that the identity, concentration, solubility, and Lewis acid-depleting characteristics of these onium salts are the primary factors governing the subtle differences among polymerizations utilizing different Lewis bases; therefore, it is crucial that future investigations within the area of quasiliving carbocationic polymerization include structural characterization of these products.

Supporting Information Available: Figures showing first-order plots, partial ATR−FTIR spectra, M_n and PDI vs monomer conversion plots, GPC chromatograms, and Arrhenius plot of $\ln(k_{app})$ vs $1/T$ for IB polymerizations. This material is available free of charge via the Internet at http://pubs.acs.org.

References and Notes

(1) Faust, R.; Kennedy, J. P. *J. Polym. Sci., Part A: Polym. Chem.* **1987**, *25*, 1897.
(2) Kaszas, G.; Puskas, J. E.; Chen, C. C.; Kennedy, J. P. *Polym. Bull.* **1988**, *20*, 413.
(3) Kaszas, G.; Puskas, J. E.; Kennedy, J. P.; Chen, C. C. *J. Macromol. Sci., Pure Appl. Chem.* **1989**, *A26*, 1099.
(4) Iván, B. *Makromol. Chem., Macromol. Symp.* **1993**, *67*, 311.
(5) Matyjaszewski, K. *Macromolecules* **1993**, *26*, 1787.
(6) Szwarc, M. *Makromol. Chem., Rapid Commun.* **1992**, *13*, 141.
(7) Kennedy, J. P.; Iván, B. *Designed Polymers by Carbocationic Macromolecular Engineering: Theory and Practice*; Hanser Publishers: Munich, 1991; pp 59−78.
(8) Kaszas, G.; Puskas, J. E.; Chen, C. C.; Kennedy, J. P. *Macromolecules* **1990**, *23*, 3909.
(9) Zsuga, M.; Kennedy, J. P. *Polym. Bull.* **1989**, *21*, 5.
(10) Iván, B. *Macromol. Symp.* **1998**, *132*, 65.
(11) Plesch, P. H. *Makromol. Chem., Macromol. Symp.* **1992**, *60*, 11.
(12) Penczek, S. *Makromol. Chem., Rapid Commun.* **1992**, *13*, 147.
(13) Gyor, M.; Wang, H.-C.; Faust, R. *J. Macromol. Sci., Pure Appl. Chem.* **1992**, *A29*, 639.
(14) Fodor, Z.; Gyor, M.; Wang, H.-C.; Faust, R. *J. Macromol. Sci., Pure Appl. Chem.* **1993**, *A30*, 349.
(15) Pernecker, T.; Kennedy, J. P. *Polym. Bull.* **1991**, *26*, 305.
(16) Pernecker, T.; Kennedy, J. P.; Iván, B. *Macromolecules*, **1992**, *25*, 1642.
(17) Pernecker, T.; Kennedy, J. P. *Polym. Bull.* **1992**, *29*, 27.
(18) Pernecker, T.; Kelen, T.; Kennedy, J. P. *J. Macromol. Sci., Pure Appl. Chem.* **1993**, *A30*, 399.
(19) Deák, Gy.; Zsuga, M.; Kelen, T. *Polym. Bull.* **1992**, *29*, 239.
(20) Matyjaszewski, K.; Sawamoto, M. Controlled/Living Carbocationic Polymerization. In *Cationic Polymerizations: Mechanisms, Synthesis, and Applications*; Matyjaszewski, K., Ed.; Marcel Dekker: New York, 1996; p 370.
(21) Matyjaszewski, K.; Sigwalt, P. *Polym. Int.* **1994**, *35*, 1.
(22) Storey, R. F.; Chisolm, B. J.; Brister, L. B. *Macromolecules* **1995**, *28*, 4055.
(23) Puskas, J. E.; Kaszas, G.; Litt, M. *Macromolecules*, **1991**, *24*, 5278.
(24) Pernecker, T.; Kennedy, J. P. *Polym. Bull.* **1992**, *29*, 21.
(25) Storey, R. F.; Donnalley, A. B. *Macromolecules* **1999**, *32*, 7003.
(26) Mayr, H.; Roth, M.; Deters, M. *Macromolecules* **1997**, *30*, 3965.
(27) Roth, M.; Mayr, H. *Macromolecules* **1996**, *29*, 6104.
(28) Schlaad, H.; Kwon, Y.; Sipos, L.; Faust, R.; Charleux, B. *Macromolecules* **2000**, *33*, 8225.
(29) Plesch, P. H. *Macromolecules* **2001**, *34*, 1143.
(30) Storey, R. F.; Choate, K. R., Jr. *Macromolecules* **1997**, *30*, 4799.
(31) Storey, R. F.; Donnalley, *Macromolecules* **2000**, *33*, 53.
(32) Kaszas, G.; Puskas, J. E. *Polym. React. Eng.* **1994**, *2*, 251.
(33) Puskas, J. E.; Lanzendörfer, M. G. *Macromolecules* **1998**, *31*, 8684.
(34) Paulo, C.; Puskas, J. E.; Angepat, S. *Macromolecules* **2000**, *33*, 4634.
(35) Storey, R. F.; Curry, C. L.; Brister, L. B. *Macromolecules* **1998**, *31*, 1058.
(36) Storey, R. F.; Curry, C. L.; Hendry, L. K., submitted to *Macromolecules*.
(37) Fodor, Z.; Bae, Y. C.; Faust, R. *Macromolecules* **1998**, *31*, 4439.
(38) Held, D.; Iván, B.; Müller, A. H. E.; de Jong, F.; Graafland, T. *ACS Symp. Ser.* **1997**, *665*, 63.
(39) Storey, R. F.; Curry, C. L. *Polym. Prepr. (Am. Chem. Soc., Div. Polym. Chem.)* **1999**, *40* (2), 954.
(40) Perrin, D. D.; Armarego, W. L. F. *Purification of Laboratory Chemicals*; Pergamon Press: New York, 1988; p 357.
(41) Storey, R. F.; Donnalley, A. B.; Maggio, T. L. *Macromolecules* **1998**, *31*, 1523.
(42) Puskas, J. E.; Lanzendörfer, M. G.; Peng, H.; Michel, A.; Brister, L. B.; Paulo, C. Kinetics of the Living Polymerization of Isobutylene. In *Ionic Polymerizations and Related Processes*; Puskas, J. E., Ed.; Kluwer Academic: Dordrecht, The Netherlands, 1999.
(43) Puskas, J. E.; Lanzendörfer, M. G.; Pattern, W. *Polym. Bull.* **1998**, *40*, 55.
(44) Balogh, L.; Faust, R. *Polym. Bull.* **1992**, *28*, 367.
(45) Masure, M.; Sigwalt, P. *Makromol. Chem., Rapid Commun.* **1983**, *4*, 269.
(46) Bennevault, V.; Peruch, F.; Deffieux, A. *Macromol. Chem. Phys.* **1996**, *197*, 2603.
(47) Kennedy, J. P.; Smith, R. A. *J. Polym. Sci., Part A: Polym. Chem.* **1980**, *18*, 1523.
(48) Nagy, A. *Polym. Bull.* **1985**, *14*, 259.
(49) Reference 20, p 268.
(50) Storey, R. F.; Choate, K. R., Jr. *J. Macromol. Sci., Pure Appl. Chem.* **1997**, *A34*, 1195.

(51) Storey, R. F.; Maggio, T. L. *Macromolecules* **2000**, *33*, 681.
(52) Geacintov, C.; Smid, J.; Swarc, M. *J. Am. Chem. Soc.* **1961**, *83*, 1253; **1962**, *84*, 2508.
(53) Szwarc, M. *Carbanions, Living Polymers and Electron-Transfer Processes*; Wiley: New York, 1968, p 408.
(54) Fehérvári, A.; Kennedy, J. P.; Tüdos, F. *J. Macromol. Sci., Chem.* **1981**, *A15*, 215.
(55) Iván, B.; Kennedy, J. P. *Macromolecules* **1990**, *23*, 2880.
(56) Matyjaszewski, K.; Pugh, C. Mechanistic Aspects of Cationic Polymerization of Alkenes. In *Cationic Polymerizations: Mechanisms, Synthesis, and Applications*; Matyjaszewski, K., Ed.; Marcel Dekker: New York, 1996; pp 205−206.
(57) Reference 56, p 154.

MA0016432